

Crustal refraction survey using sonobuoys on JQZ-TN272

Stephen Swift, Adrienne Oakley, Jinchang Zhang (Sam), and Dan Lizarralde

During seismic operations on TN272, 50 sonobuoys were deployed at 16 km intervals and their radio signal recorded to provide data with which to investigate the possible presence of abnormal Jurassic crustal structure produced by volcanism during the Cretaceous.

Equipment

Fifty sonobuoys purchased from Ultra Electronics (Dartmouth, Nova Scotia) were stored in their wood shipping container at the aft end of the staging bay on the main deck. The receivers were modified military-type DIFAR AN/SSQ-53D(3) omnisensitivity sonobuoys manufactured in November 2010 (Ultra Electronics PO E112980). The manufacturer rates the operating frequency band to 5-2,400 Hz. Figure 1 shows that the frequency response of the 'modified' 53D sonobuoys provided by the manufacturer peaks at 40-50 Hz with 10 db down points at 9 Hz and 310 Hz.

Radio signals were received on the ship with a Sinclair Model SY2062-SF2SNM(C) antenna. This model is a dual stacked, 12 dBd, center mount, 152-159 MHz YAGI antenna. The antenna was mounted on 1.5 in diameter pipe at 10' height above the starboard end of the flying bridge at about 9 m off the ship's centerline along frame 57. The flying bridge is 54 feet (16.5 m) above sea level, so the antenna is mounted at about 64 feet (19.5 m) above sea level. A Yaesu Model G-450A rotation motor was installed as part of the antenna mount and cabled to a controller box in the computer lab, so the antenna could be rotated if we suspected strong currents carried the sonobuoys off the ship track. Appendix 1 includes pictures of the antenna installation.

The antenna signal was cabled to the computer lab and into a WinRadio Model WR-G39WSBe receiver, which could be controlled by WinRadio software on a Dell PC. The demodulated signal was run in series through two Krohn-Hite Model 3700 analog filters each set to pass 1-150 Hz with zero gain. The filtered output was split so the signal could be recorded as an auxiliary channel by the multi-channel seismic (MCS) system and as channel one by a Ref Tek RT130. The airgun trigger signal from the MCS fire-control system was recorded as channel two of the Ref Tek 130. The RT130 digitized both signals at 500 Hz and recorded them in Ref Tek compressed format. A gain of 32 (high) was applied to the sonobuoy signal; a gain of one (low) was applied to the gun trigger. We switched from Ref Tek 130 S/N 991F to S/N 9873 between seismic lines 1 and 2. The MCS recorded seismograms at 1000 Hz with a pre-amp gain of 18 db for streamer channels and 0 db gain for the auxiliary channels (including the sonobuoy channel). No frequency filtering was done by the MCS system prior to digitizing for either the streamer or the sonobuoy channels.

GPS time and ship location were continuously recorded by the Ref Tek 130 using a feed from a Garmin 16-HVS GPS receiver (labeled "Ref Tek RT 130 GPS-02 S/N 6509") mounted on the 02 deck about one meter to port of the centerline of the ship on ship frame number 91 at an elevation of 45 feet (13.7 m) above sea level. Appendix 2 includes pictures of the RefTek GPS installation. Test of the integrity of the system were made while at the dock and while underway prior to operations using a test sonobuoy disabled for us by the manufacturer.

Processing

After the airguns were turned off at the end of each seismic line, the Ref Tek 130 was allowed to record data for an additional 10-15 minutes before terminating acquisition. Disk utilization was noted and the Ref Tek was left powered for an additional 0.5-1 hr before the power was turned off and the current compact flash card removed. Software provided by PASSCAL (Neo) was used to copy the data off the card onto a MacBook using a Kingston FCR-HS219/1 card reader. The compressed data in zip files created by Neo were reformatted to MiniSeed using PASSCAL software (rt2ms). Another PASSCAL program (pql) was used to inspect the time series and compute spectra. ProMAX seismic processing package (Landmark) was used to make a record section from the auxiliary channel of the segd file recorded by the MCS system. We plotted the sections with GMT, and a screen capture was used to print the sections. Figure 2 shows a sample record section of SB#3. Appendix 3 contains a copy of all plots. All data files were archived to a 500 Gb Lacie drive.

Sound Speed Profiles

Knowledge of vertical sound speed variations in water will be useful in ray-trace modeling of sonobuoy seismograms. Depth profiles of sound speed were obtained from both XBT temperatures and from temperature, salinity, and pressure measured by a SeaBird SBE 49 CTD mounted on Sentry during dives along the survey line. Table 1 contains details of the XBTs, and Figure 3 shows a map of the XBT stations. The acquisition software computed sound speed assuming a constant salinity (given in Table 1). Sound speed variations with depth (Figure 4) follow the trend from gridded historic data (S. Levitus, Climatological atlas of the world ocean, NOAA Prof. Paper 13, 173 pp., 1982, obtained using MBSysstem) except where they systematically exceed the historic average by ~5 m/s in a prominent well-mixed layer in the upper 100 m.

To compute depth and sound speed for the SBE 49 data from Sentry, we ran Matlab scripts written by P. Morgan (CSIRO) using algorithms from Fofonoff and Millard (Algorithms for computation of fundamental properties of seawater, UNESCO Tech. Paper in Marine Science 44, 53 pp., 1983). Initial results showed that salinity more often appeared to be reasonable during Sentry's ascent than during her descent - probably due to slow flushing of tubing leading to the salinity sensor at the start of the dives and, perhaps, warming of the sensor by the thermal mass of Sentry. Table 2 contains dive locations, and Figure 5 shows locations of the recovery positions of Sentry, which are a good approximation for the location of the ascent CTD profiles. Dives 130-131 are shallow water test dives. Figure 6 shows profiles of temperature, salinity, and sound speed. Conductivity values during dive 130 remain near 0.02-0.03 throughout the dive indicating that the sensor failed; sound speed values for this dive are unreasonably low. The salinity profiles for dives 128 and 134 are anomalous also indicating problems with the sensor. As a result, values of sound speed for dives 128 and 134 are untrustworthy. With two exceptions, sound speed profiles from Sentry follow Levitus. (1) In the upper limb of the sound speed channel between 250 and 750 m depth, sound speed from Sentry is up to 10 m/s slower than Levitus. (2) Sound speed is 5-10 m/s faster than Levitus in a well-mixed layer in the upper 60 m. There is some indication that the thickness and sound speed of the well-mixed layer increase during the course of the survey, perhaps indicating turbulent mixing caused by 20-30 knt winds encountered and solar warming of the sea surface.

Geometry

Knowing the range from each airgun shot to the active sonobuoy receiver is essential to interpret the sonobuoy seismograms. Range is computed from the location of each shot and the location of the sonobuoy at launch assuming that the sonobuoy does not drift. For this experiment, the location of each airgun shot can be determined using the offset of the airgun array from the point on the ship to which the P-code GPS fixes are referenced. Appendix 4 contains figures showing the offsets from the airguns to the Inertial Motion Unit (IMU). The IMU is located along the starboard wall of the engineers' office on the platform deck (ship frame 53, 1.5 m port of the centerline). The NEMA strings recorded in the seismic segd headers and provided to Swift in ascii files for each line ("TN272*.Nav.txt") contain P-code GPS locations from the "PosMV" navigation system after being shifted to the location of the IMU. The ship locations recorded in the shipboard "DAS" data logging files and recorded by the sonobuoy watchstanders at the time of launch come from the "C-Nav" P-code GPS system. Figure 7 shows the schematic locations of the key spots on the ship relevant to sonobuoy operations, and Table 3 provides the offsets to the IMU. It is important to note that the watchstanders recorded the time that the sonobuoy hit the water surface, so a further correction must be applied. Sonobuoys launched from the main deck (SB# 1-3) landed about 1.5 sec after being thrown; they hit the water about 3 m aft of their launch position (assuming a ship speed of 4 knts – 2 m/sec) and 2-3 m outboard. Sonobuoys launched from the 02 deck (SB# 4-5 and 7-50) landed about 3 sec after being thrown; they hit the water about 6 m aft of their launch position and 3-4 m outboard. The one sonobuoy thrown from the bridge deck (SB# 6) landed about 4 sec after being thrown; it hit about 8 m aft of its launch position and 3-4 m outboard.

Launch Protocol

Prior to start of seismic operations, power was turned on to the Krohn-Hite filters, the radio receiver, Ref Tek 130, and PC. The sonobuoy channel was selected using the Win Radio software on the PC, and acquisition was started on the Ref Tek 130. Enough sonobuoys for the up-coming seismic line were removed from the shipping container and stored on a table top in the main lab. Operations typically required three people: one to carry and throw the sonobuoy and a radio operator to call back to the lab at the instant the buoy hit the water, and a data logger positioned by a ship data screen in the computer lab. Sonobuoys were removed from their plastic shipping tubes, and the wind flap and parachute netting were disconnected. The radio channel, buoy life, and hydrophone depth were programmed. The WinRadio display usually showed higher background noise on channels above channel 48 (>142.000 Mhz), so we used only channels 32-48 (136.000-142.000 Mhz). The scuttle time for the buoys was always set to 8 hrs (choices – 0.5, 1, 2, 4, 8 hrs). The hydrophone depth could be set to d1 (100' – 30.5 m), d2 (200' – 61.0 m), d3 (400' – 122 m), or d4 (1000' – 305 m). Buoys were thrown over the starboard rail on the main deck, the starboard 02 deck, the bridge deck (once), or the port 02 deck (Figure 7, Table 3). The float usually emerged within 10-15 sec and was observed to drift aft to the outboard of the streamer. Buoys were launched at 16 km intervals starting at the beginning of each seismic line.

Seismic Operations

Table 4 provides details of the sonobuoy deployments; Table 5 gives the MCS line number and shot number at the launch and termination of each buoy. Figure 8 shows the locations of launch positions on a map of satellite-derived bathymetry. Lines 1-2 were shot at a ship's heading of $\sim 218^\circ$. The azimuth of the survey line changed to $\sim 225^\circ$ between sonobuoys 24 and 25. For buoys that returned a signal, Figure 9 shows the decay with time in the amplitude of the Win Radio signal on the transmission channel. Although very short spikes of high amplitude appear during every shot, we recorded the background amplitude. Thus, Figure 9 probably represents the strength of the sonobuoy's carrier signal. Most buoys follow a pattern of amplitude decay with time that resembles a $1/r^2$ pattern. Sonobuoys 5 and 24 had unusually weak signals throughout the ~ 2 hours that we monitored them.

During seismic line 2, which was exceptionally long, the sleep function on the PC would activate and hang up the computer. When this occurred, we shut down the PC using the power switch before re-booting the PC and the Win Radio software. Using the PDA and the monitoring functions provided with the RT 130, we found that the receiver continued to send seismic signal to the RT 130. So, the Win Radio software is not required to operate the Win Radio receiver itself. We disabled the sleep function before later seismic operations.

Line 1

All four buoys were launched with the hydrophone depth set to D1 (30.5 m). ADCP surface currents were consistently 1-2 knots to the SW parallel to the shooting line; winds were generally 8-12 knots to the west and to the west-northwest. The sonobuoy signal monitored by the RT130 for SB 1 appeared to have exceptionally better signal-to-noise character than for SBs 2-4. However, the MCS channel gather shows that only the first 5% of the shots for SB 1 were recorded on the MCS auxiliary channel. In retrospect, it is likely that inexperience lead us to interpret a persistent random noise chirp as a clean airgun signal. If this interpretation is true, then Sonobuoy 1 must be added to the list of failed buoys (Table 4). Figures 10 and 11 show a sample time series and a spectrum of the noise chirp recorded after the airguns had been turned off at the end of Line 1. The signal is predominantly a 1 Hz oscillation that decays with time. It is present throughout the sonobuoy data. The amplitude of the chirp does not appear to vary during the survey indicating that the chirp is not transmitted from the buoys whose signal decays with time (Figure 9). The noise source must be on the ship).

Line 2

Thirteen sonobuoys were launched, but only 8 buoys provided adequate signal. No seismic signal was seen on SB 11. We initially observed good data on the MCS monitor for SBs 7, 8, 10 and 17, but the signal terminated after ~ 5 minutes. On all five bad buoys, the amplitude seen in the WinRadio display jumped at the start and decayed normally with time indicating that the buoy transmitter sending the carrier frequency functioned normally. It is possible that the connection between the hydrophone at depth and the transmitter at the sea surface was cut or damaged by a wing of one of four birds mounted on the streamer. But no wires were found when the birds were recovered at the end of the line. Despite the lack of debris, our experience at the beginning of Line 7 indicates that the cause of premature termination of sonobuoy data was indeed cutting of the hydrophone

wire by a streamer bird. Interestingly, the 1-2 sec long noise chirp centered at 1 Hz continued to appear even when the seismic signal did not, so the source of the chirp is unlikely to be in the marine environment. Moreover, the chirp does not stop when the Knudsen echosounder is turned off.

A large time gap occurred in MCS shooting between the end of Line 2 Part 1 (04:43:28/321) and Part 2 (05:01:06/321) when the ship drifted off the shooting line pre-set in the MCS navigation software (HyPack). This gap happened during SB#7, for which there were no seismograms recorded (Table 4).

At the beginning of Line 2, Hydrophone depths D2 and D3 were used on SBs 5-11 to try to reduce noise seen SBs 2-4, which were deployed using D1. We were not able to detect a change in noise level, although we had no way to quantitatively compare noise levels while recording data. In despair, we switched back to D1 after the fourth bad sonobuoy and obtained good data for five sequential buoys.

Lines 7-10

The remaining 33 sonobuoys were deployed during four days of shooting (Table 4). The MCS data was broken into four segments (Lines 7-10) to allow easier processing. Recording was stopped for a few shots during these line number changes, so sonobuoy data recorded on the MCS auxiliary channel was lost (Table 5). Gaps at these breaks in line number are too short to appear in the plots of channel gathers (Appendix 3). Fortunately, recording on the RT130 was continuous. A presumed electrical short caused the airguns to shut down for ~5 minutes beginning at 00:00:30 on JD 334. The shutdown is the reason for the break between MCS Lines 10 and 10A. Since the airguns were shutdown there is a gap in sonobuoy data recorded by both the MCS and the RT130 systems. The break occurs at the end of SB 47.

Sonobuoy 18 followed the now familiar pattern from Line 2 of sending data for 4-5 minutes and then stopping. Changing hydrophone depths at the beginning of Line had produced no relief. So we moved the deployment site from the starboard 02 deck to the port 02 deck. We had no further failures, except for SB 32, which was a complete dud - no carrier frequency was seen. This success was not anticipated because both the wind and the ADCP surface current flowed from the NE to SW and, thus, moved from port to starboard. We initially thought the surface current would carry sonobuoys deployed off the port side of the ship into the airguns and streamer. Observations of the flow of water around the stern offered an explanation presented in Figure 12. Because the wind and current were constantly trying to shift the boat to the west off the shooting line, the DP system turned the orientation of the ship's bow to port. Thus, the ship's stern was turned to starboard towards from its direction of motion. The most obvious evidence of this was the deflection of the airgun and streamer tail buoys to port. The more significant effect was an asymmetric flow of water around the stern of the ship and into the wake. There was clearly more flow from the starboard side than from the port as schematically shown in Figure 12. We suggest that this flow would more often carry sonobuoys launched from the starboard side into closer proximity to the streamer than those launched from the port side. The buoys launched from the starboard side that were successful were those that were thrown farther from the ship and those that were fortunate to be thrown just when the yaw of the ship placed the launcher farthest to starboard.

Results

Sonobuoy seismograms recorded on the auxiliary channel of the MCS system were stripped from the segd files and saved in segy format by line number (Table 5). Appendix 3 contains plots of shot gathers for all sonobuoys. In order to provide an indication of sediment thickness that could be used in preliminary interpretation of the MCS reflection profiles, we picked travel times to the seafloor at vertical incidence and at the point along the wide-angle seafloor reflection where crustal energy breaks out from the seafloor. As an example, the arrows in Figure 2 show where these points occur for SB 3. This difference in time was useful in identifying laterally coherent seismic reflected energy as basement on Line 2.

The difference in travel time between the seafloor reflection at vertical incidence and at the point where refracted energy breaks out is an indication of sediment thickness. Occasionally, more than one crustal breakout could be discerned, although the early breakouts are often faint, poorly defined, confused by hyperbolic diffractions, or offset by only a small time increment from the later crustal breakout. As an example, arrows in Figure 13 show three travel times picked for SB#12 in which both a shallow and deeper crustal refraction could be identified. Picked travel times are listed in Table 6 and plotted in Figure 14 as a function of sonobuoy number and latitude at launch. Due to the uncertainties, these interpretations are preliminary and were only used to guide shipboard interpretations of the MCS records prior to formal modeling and interpretation of sonobuoy record sections in a shore lab. At the base of the figure, an arbitrary index of the amplitude of the main crustal refractor is also plotted. This scale varies from zero for buoy records in which no refracted energy could be observed to five for the strongest appearing refraction. Two refracted arrivals could be identified in six sonobuoys. Sonobuoy 12 (Figure 13) on Line 2 presents the most reliable evidence of an igneous sill layer within the sediment layer.

We also examined details of specific portions of the seismograms by plotting time series for individual shots. Spectra were computed on these segments to identify the frequencies present in various arrivals. Figure 15 shows traces and spectra for the water wave arrival recorded with a hydrophone depth of 30 m. We selected the records from three sonobuoys that had particularly long-lived direct waves and relatively low noise. These water-wave arrivals represent energy traveling nearly horizontally for 2-3 km. Unlike energy traveling vertically down to the seafloor, these arrivals may include multiple interactions with the sea surface. For all three sonobuoys, the direct arrivals include 2-3 wavelengths with relatively similar amplitudes and periods of 10-12 ms. As a result, the spectra peak at 110 Hz. The spectra are remarkably flat from 5 Hz to above 130-140 Hz. The high frequency rolloff occurs below that of the Krohn-Hite anti-alias filters (150 Hz) and is, thus, a feature of the airguns and the interaction with the sea surface rather than the filters.

To determine if the depth of the hydrophone influences the seismograms, we plotted traces and spectra in Figure 16 from three sonobuoys spaced closely along Line 2 for which three different hydrophone depths (30, 61, and 122 m) were programmed. As in Figure 15, the arrivals include 2-3 wavelengths with periods of 10-12 ms. Unlike the seismograms in Figure 15, the maximum amplitude of the 2-3 pulses increase with time shifting energy to longer wavelengths. As a result, the spectra peak below 100 Hz. Hydrophone depth appears to have little effect on either the traces or the spectra. The

spectra for seismograms recorded with the hydrophone at 30 m (sonobuoy 12) are unusual in having a shallow notch at 80-90 Hz. This notch does not appear in any of the spectra in Figure 15 that were also obtained with the hydrophone set to 30 m. Thus, the primary source of variability is unlikely to be hydrophone depth and more likely some feature of the sea surface (swell amplitude, direction) or small variations in the operation of the airguns.

To examine the sediment reflections, Figure 17 shows seismograms for three sonobuoys recorded for ~ 0.6 s after the seafloor reflection. All seismograms were obtained at short range (~ 0.4 km) with the hydrophone set to 30 m depth. The traces are remarkably similar over the initial 30 ms indicating that the down-going pulse was similar. Despite the widely varying traces after the initial 30 ms, the spectra are also remarkably similar. Thus, the notches at 30, 60, and 90 Hz are likely features of the downward traveling source signature. The high frequency roll-off occurs at about 105 Hz, which is only about 20 Hz less than the roll-off frequency of the direct wave spectra in Figures 15 and 16.

To determine if the seismograms recorded by sonobuoy hydrophone differed significantly from the processed MCS seismograms, we show in Figures 18 and 19 the near-vertical incidence seismograms from two sonobuoys with CDP stacked with the same shots from two versions of processed MCS. The most remarkable feature of these plots is the similarity between sonobuoy and the MCS traces. Clearly MCS processing improves the resolution of sedimentary reflections. But the phases of individual waveforms are very similar. Spectra of the two data sets were also similar particularly those for SB#50 (bottom frame) in which the spectral notches line up. The spectra, however, initially differed at the low frequency end. In Figure 18, the MCS data (labeled "new" in the data archives) were processed with a bandpass of 20/30-180/200 Hz, whereas in Figure 19, the MCS data (labeled "final" in the data archives) were processed with a bandpass of 5/8-180/200 Hz. Spectra computed on the former data set roll off 15-20 Hz above the low frequency end of the sonobuoy spectra (Figure 18). Test MCS plots indicated some deep reflections were better imaged when the bandpass of MCS processing was expanded downward to 8 Hz (Figure 19).

A significant goal of the sonobuoy component of the survey was to identify the depth to basement and any igneous sills within the sediment sections. Shore-based processing will include efforts to better image arrivals that reveal the nature of basement features. To assist this effort, we more closely examined the refracted arrivals in three sonobuoys from which these arrivals were relatively strong. Time series and spectra for 0.45 sec intervals in Figure 20 show that the crustal refracted arrival comprises frequencies in the 10-15 Hz band. Time did not allow further examination of the features of the sonobuoy data in this passband.

Figures

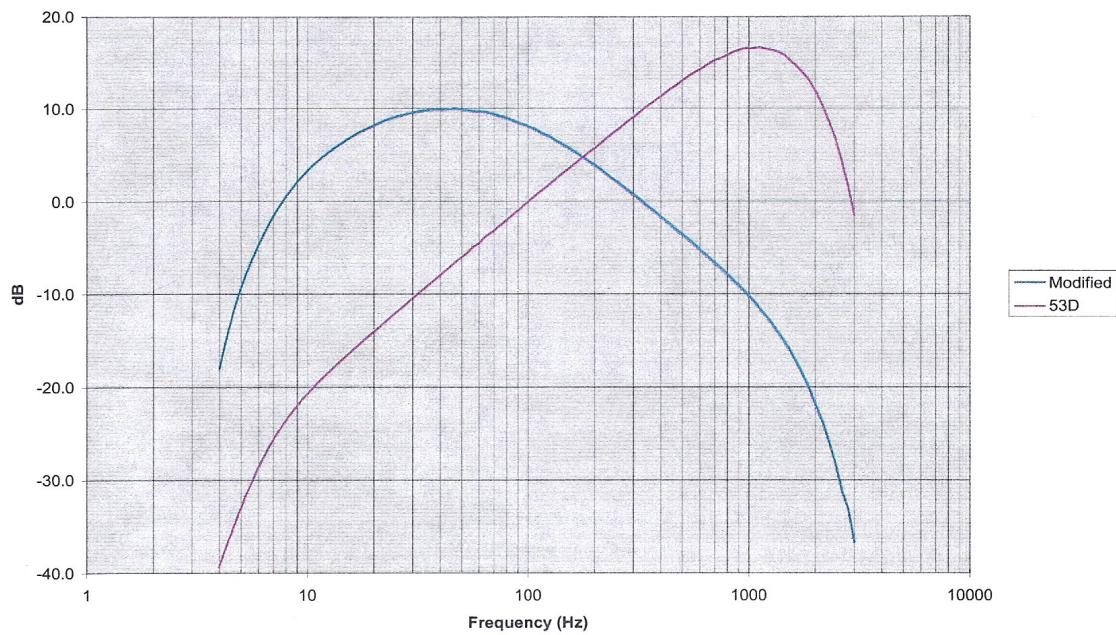


Fig. 1. The blue curve shows the frequency response of the modified 53D(3) sonobuoy provided by the manufacturer. Note that the 10 db down points occur at 9 Hz and 310 Hz. The violet curve shows the response of the standard 53D(3) sonobuoy.

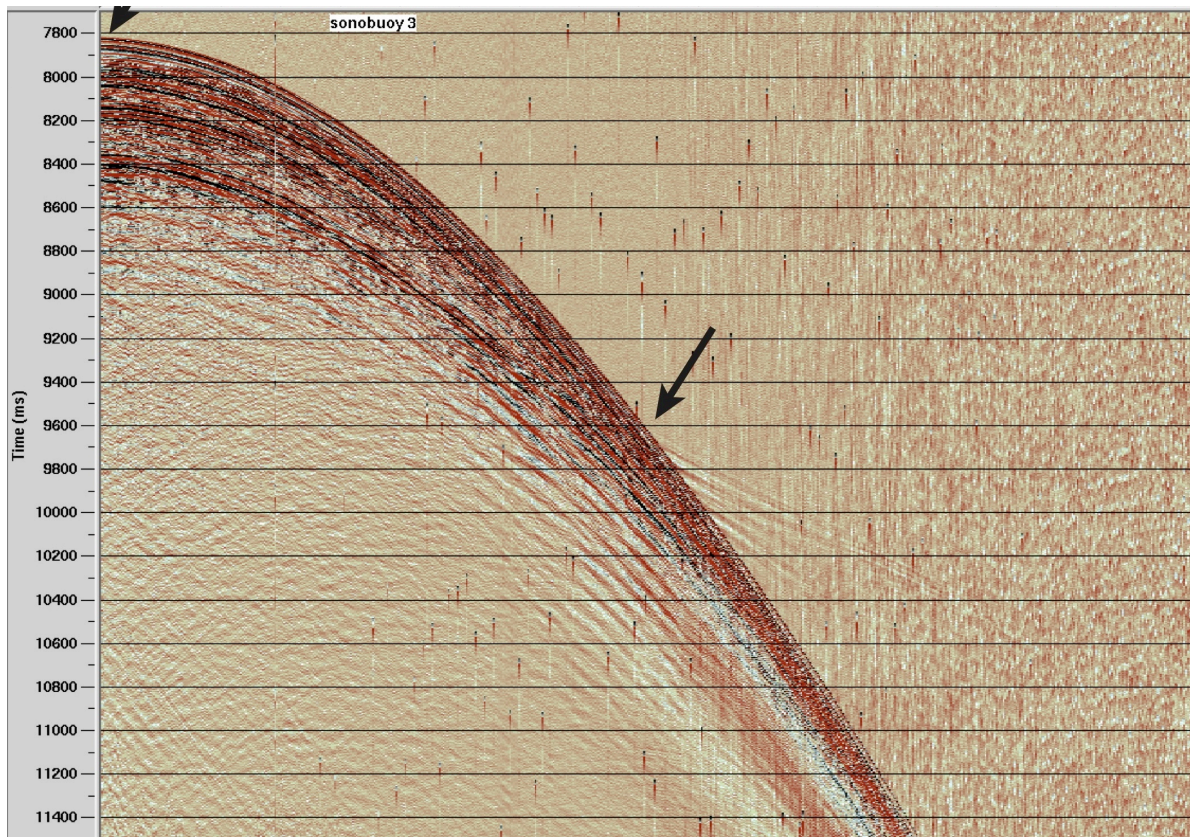


Fig. 2. A screen dump of the auxiliary channel record section for SB#3 shows a particularly well-defined sediment sequence. Arrows indicate the travel time at which we picked the vertical incidence seafloor arrival and the break out of the crustal refraction from the wide-angle seafloor reflection.

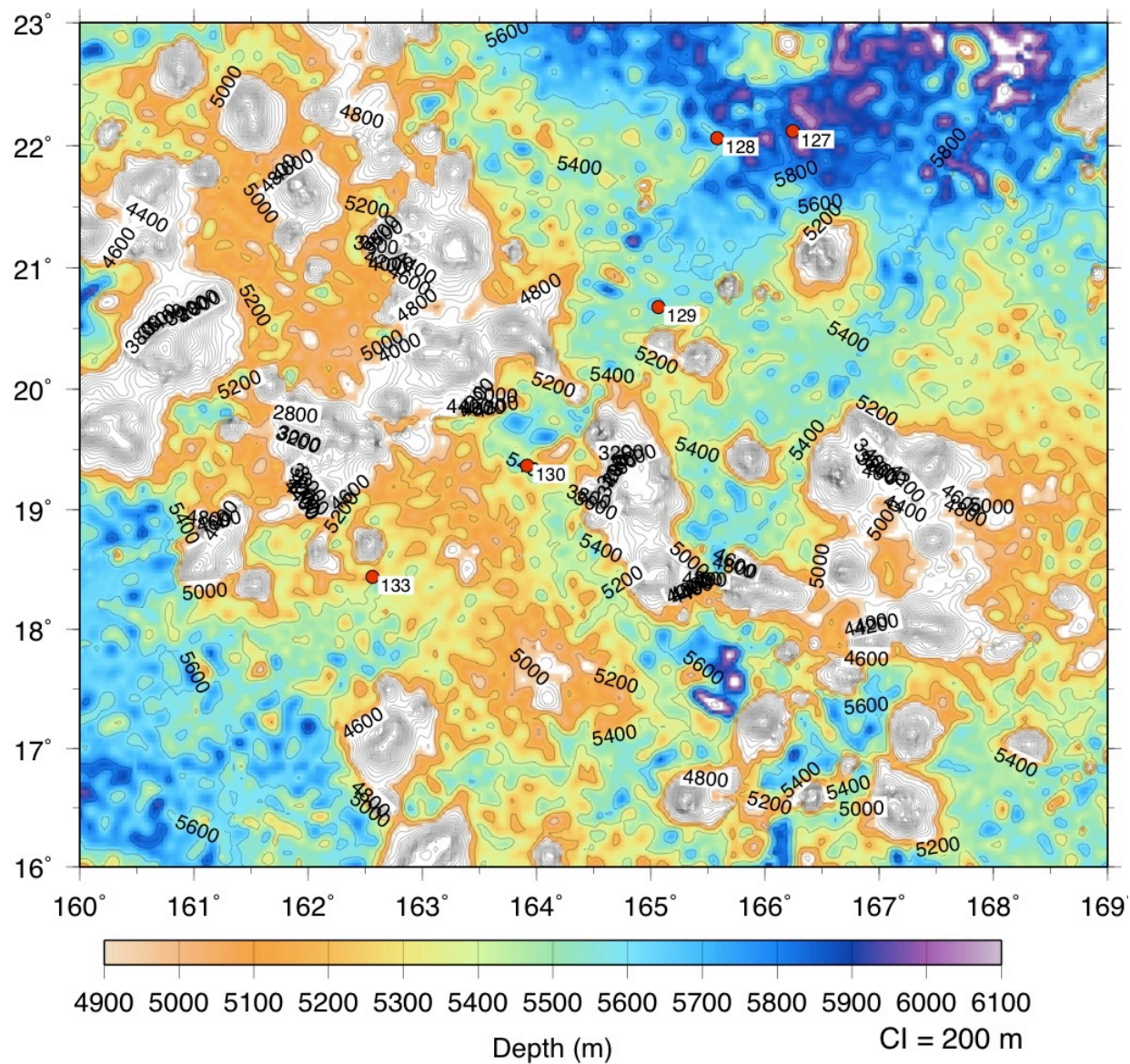


Fig. 3. Bathymetry map shows locations of XBT profiles collected on TN272. XBTs are labeled by sequence number. Table 1 provides location details.

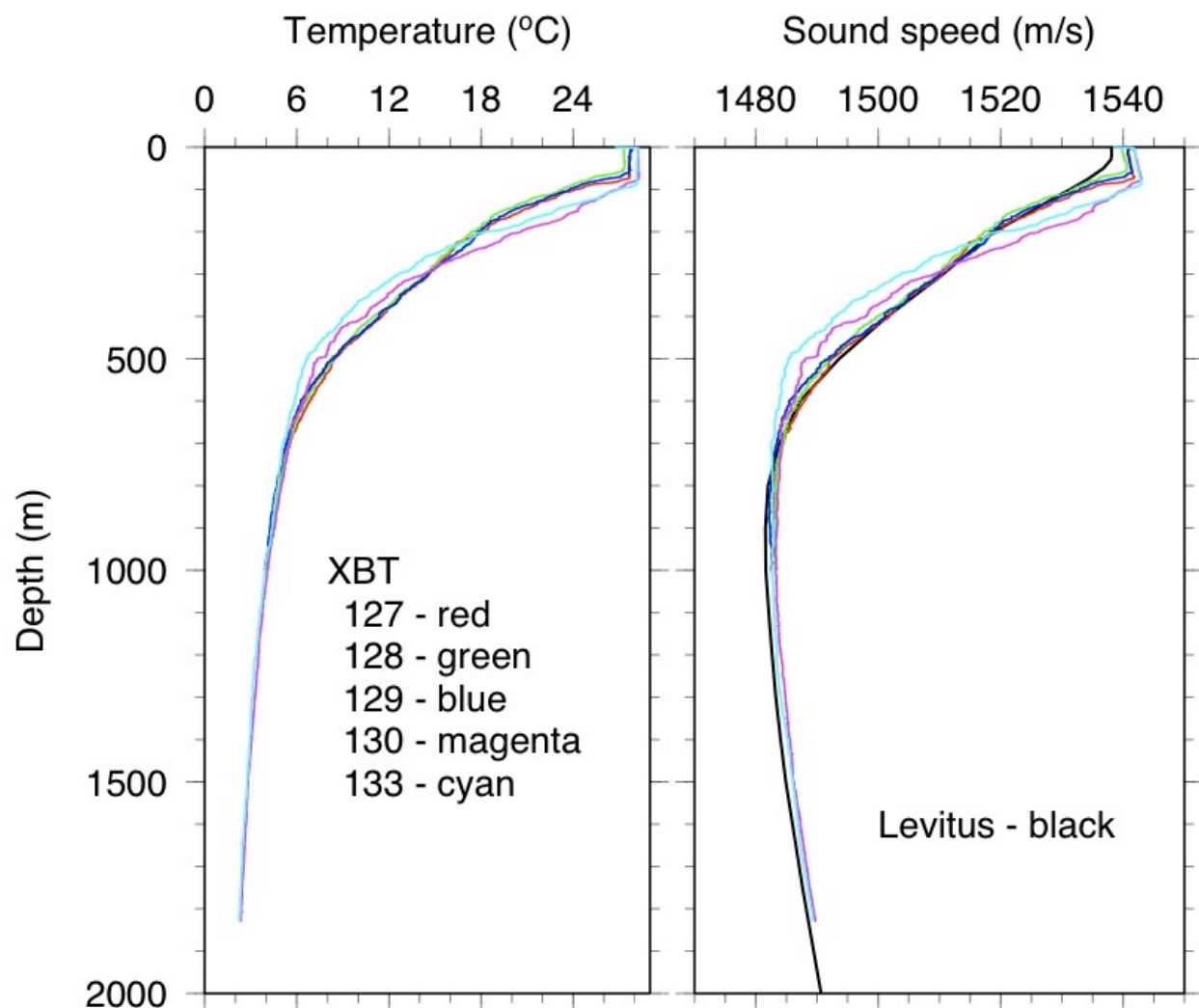


Fig. 4. The acquisition software for the ship's XBT system computed sound speed from in-situ temperature using a single assumed salinity. Sound speed profiles from four XBTs are within 1-2 m/s of the historic gridded average from Levitus (1982, black line) except within the upper limb of the sound channel and within the well-mixed layer. Locations shown in Table 1 and Figure 3.

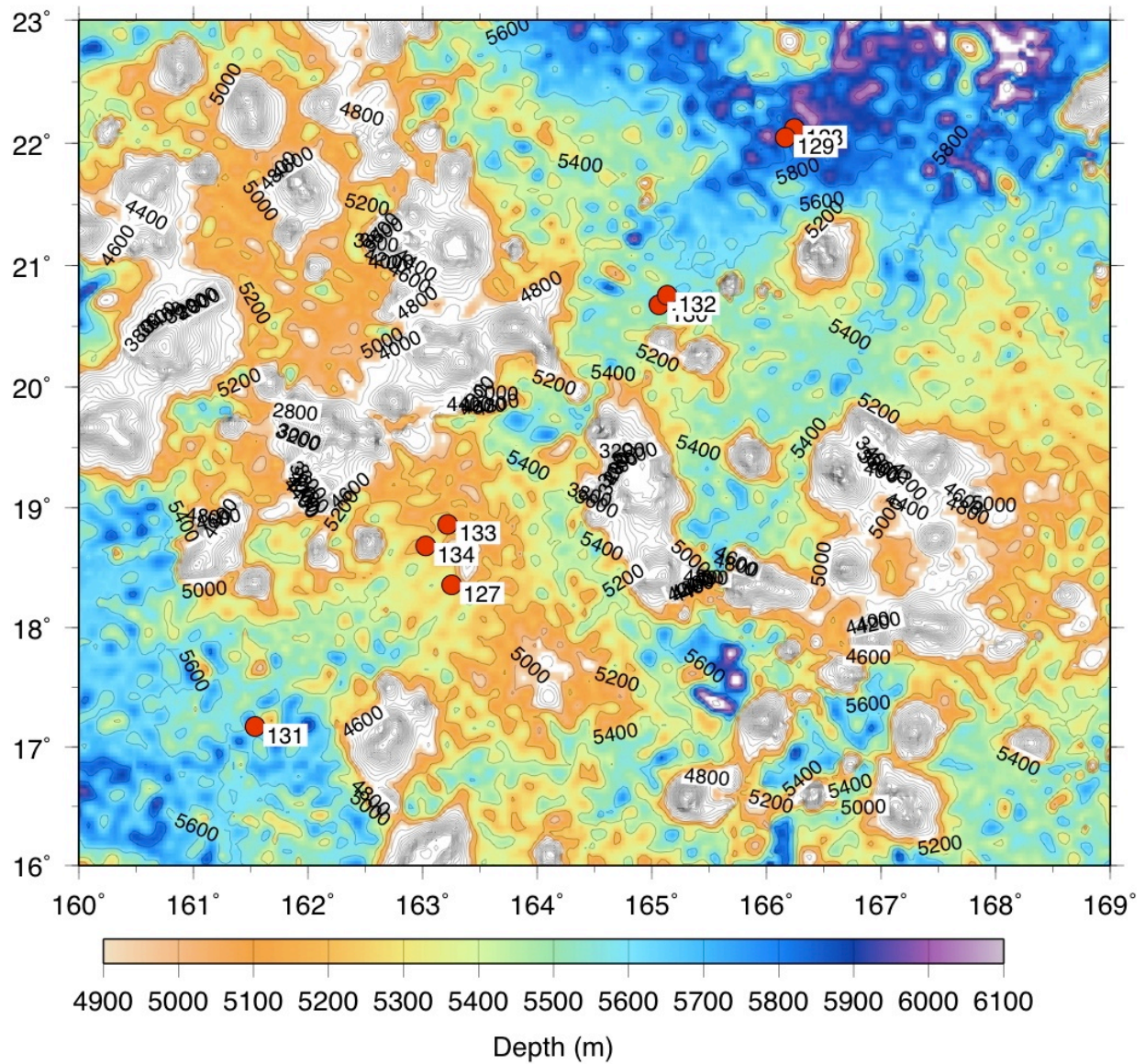


Fig. 5. The recovery positions of Sentry dives provides a close approximation to the location of CTD profiles recorded during the ascent of Sentry. Locations labeled with the Sentry dive number.

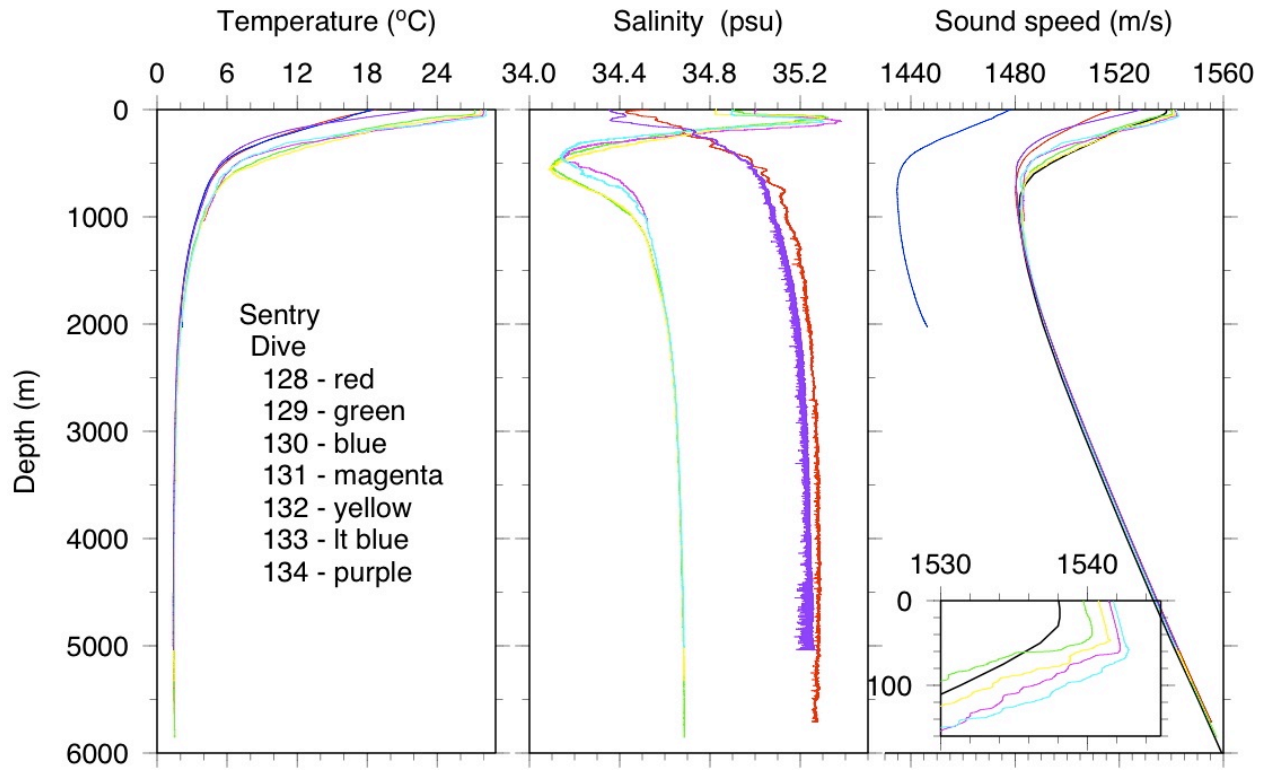


Fig. 6. Profiles of in-situ temperature and salinity are from the SBE 49 CTD on Sentry. Table 2 provides locations, and Figure 5 shows the locations on a bathymetry map. Depth and sound speed were computed using CSIRO Matlab scripts. Poor quality salinity values cause the large variations in sound speed.

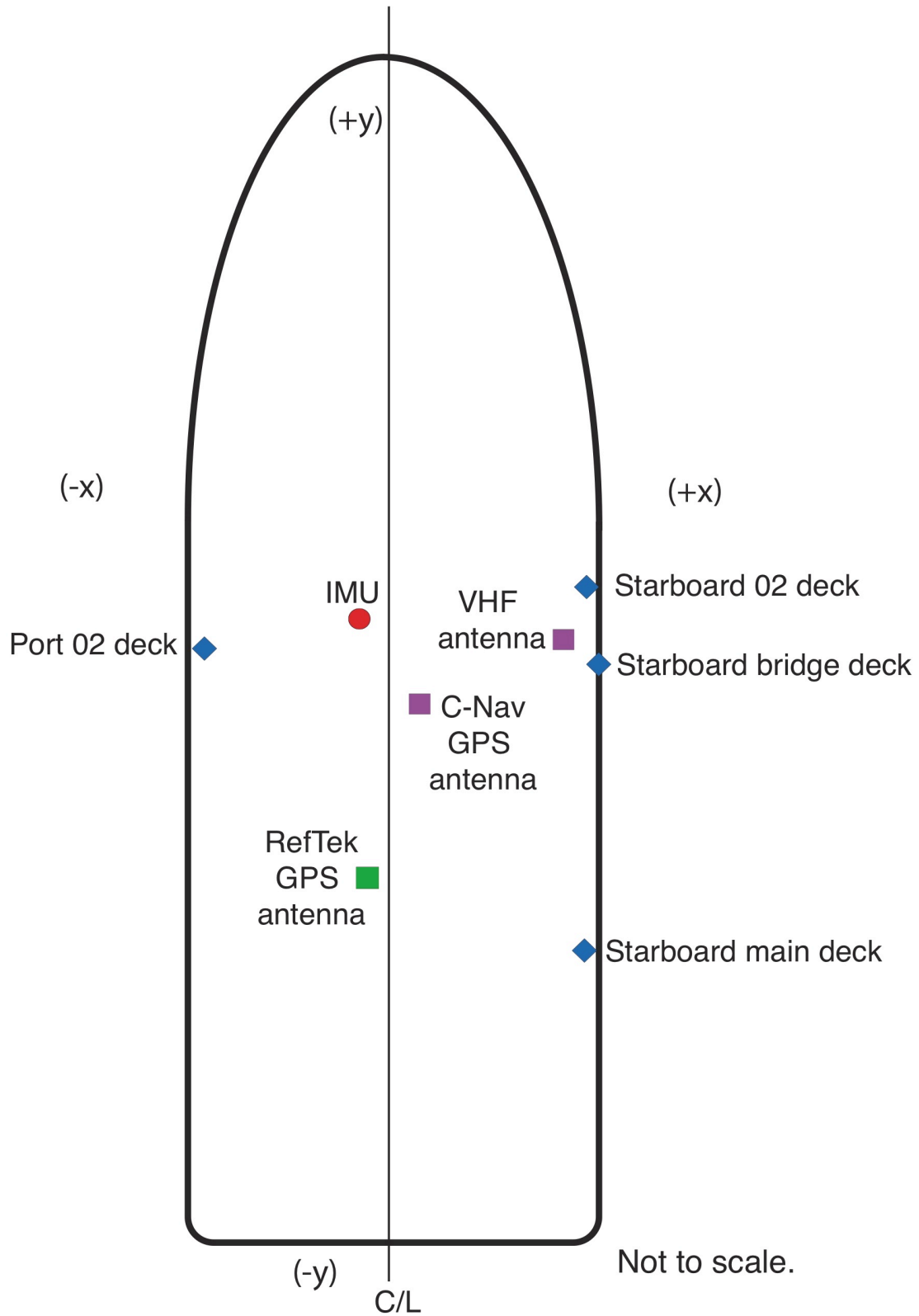


Fig. 7. The locations of the sonobuoy launch sites and the RefTek GPS unit are schematically shown in relationship to the IMU. The ship's PosMV GPS system provided navigation strings to the segd headers after correction to the IMU.

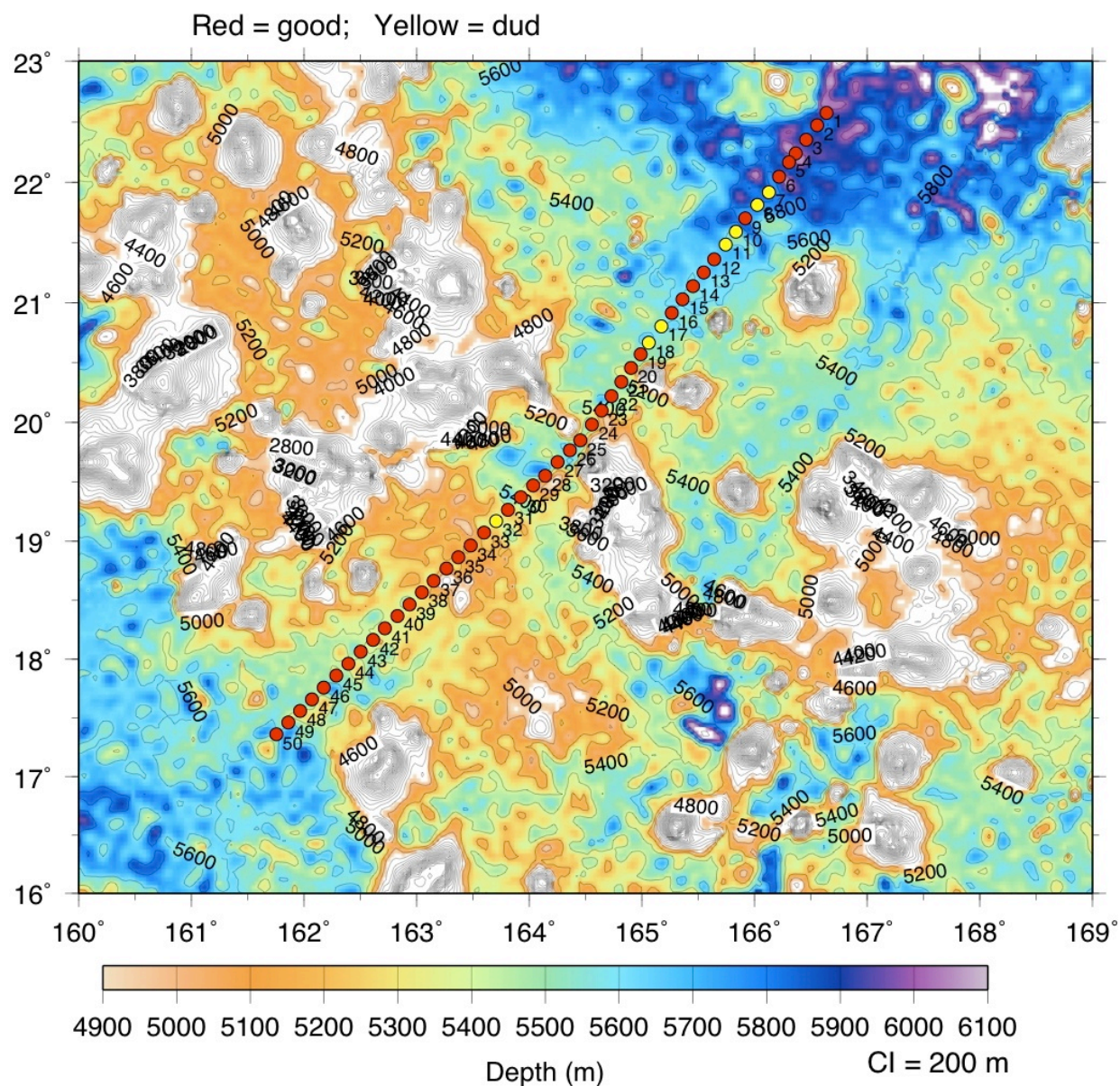


Fig. 8. Launch positions for the 50 sonobuoys are shown on a map of satellite-derived bathymetry.

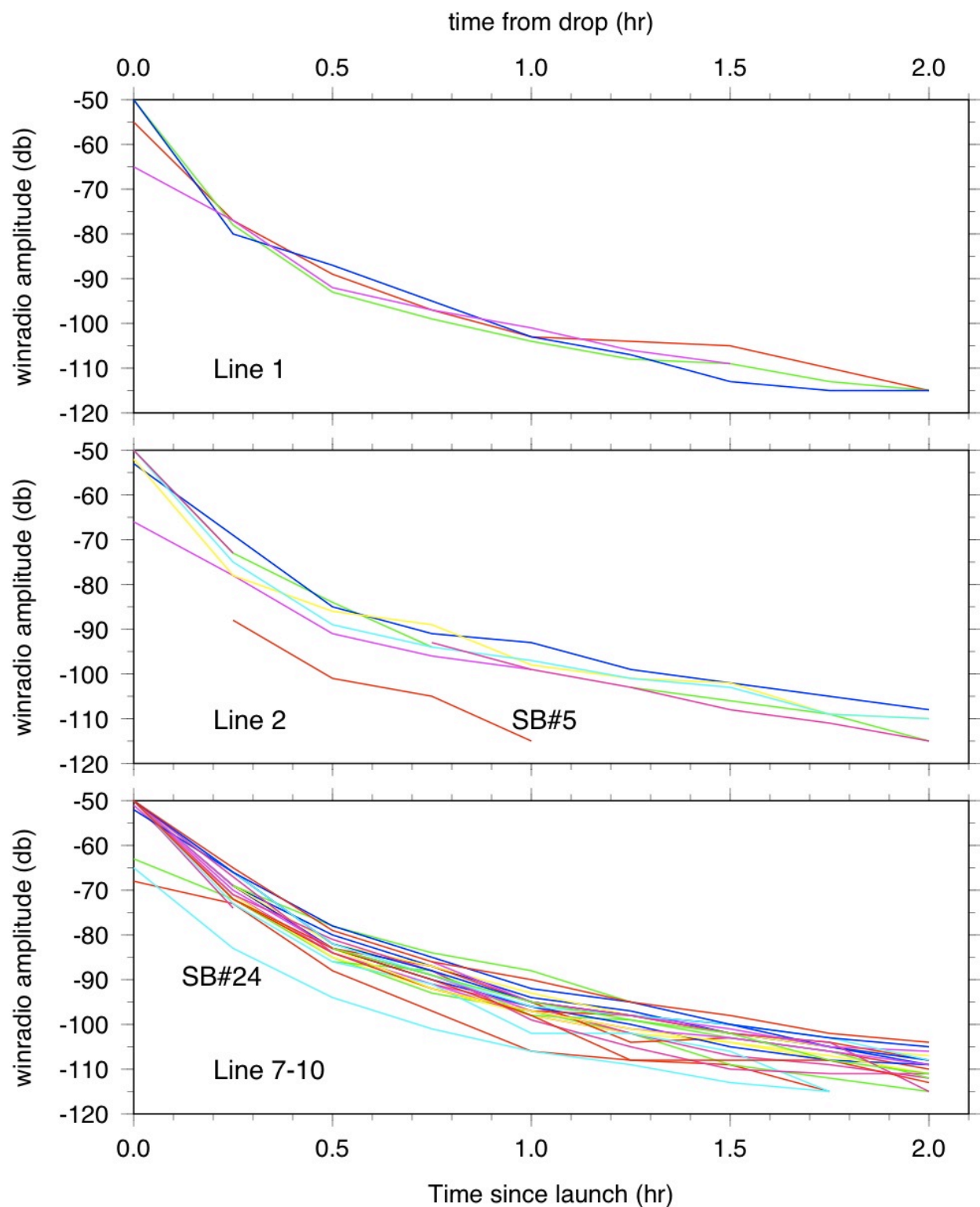


Fig. 9. The amplitude of the carrier signal as displayed on the Win Radio monitor decays as range of the buoy increases. The signals from Sonobuoys 5 and 24 were unusually weak.

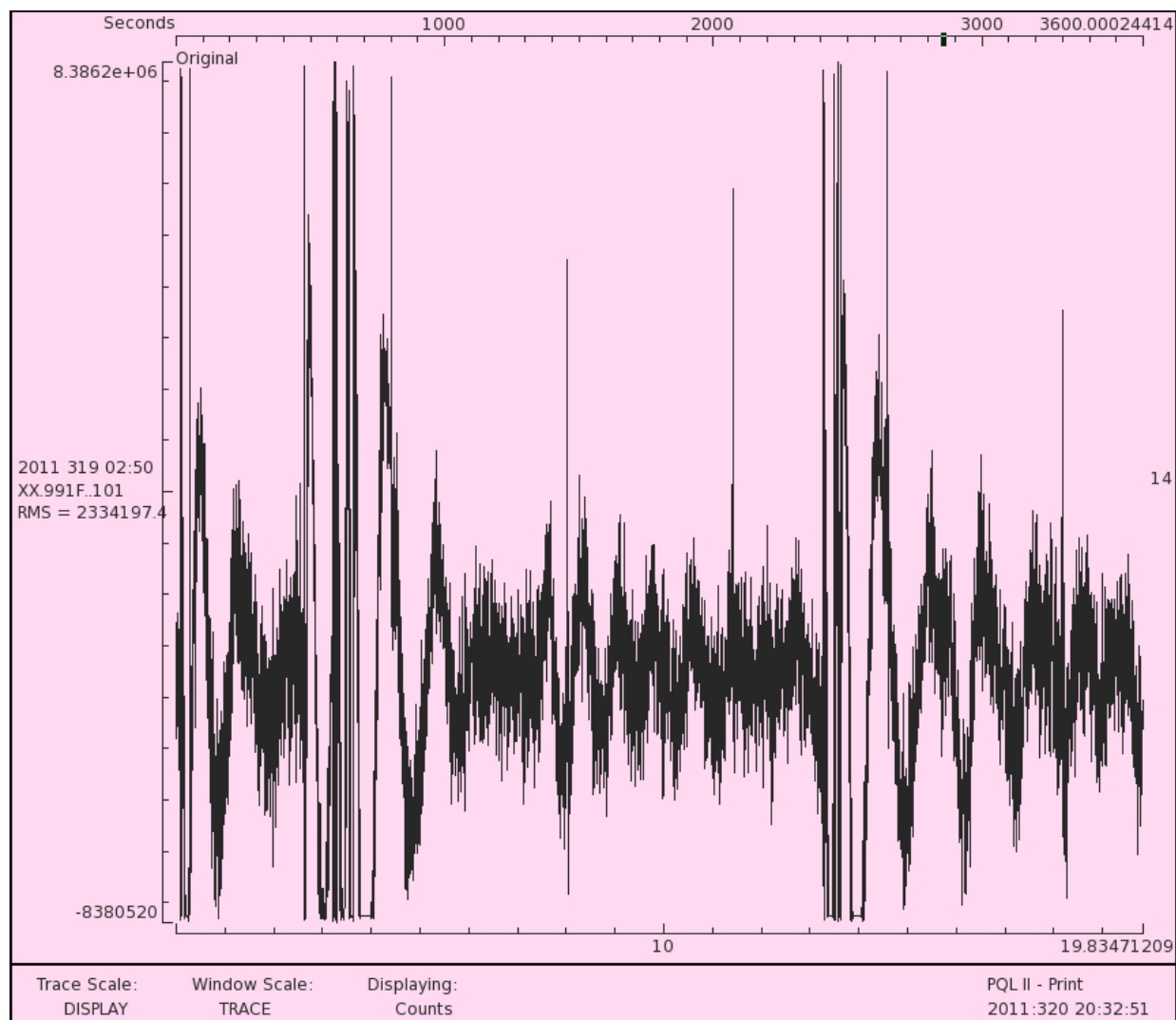


Fig. 10. A ~20 sec long time series plot of the sonobuoy channel recorded by the RT130 after the airguns had been shut down at the end of Line 1 shows two examples (at 2.5-6 sec and 13-17 sec) of the noise chirp that afflicts the entire sonobuoy data set. The period of the primary oscillation is one second, which appears as a peak at 1 Hz in a spectrum of a chirp interval in Figure 11.

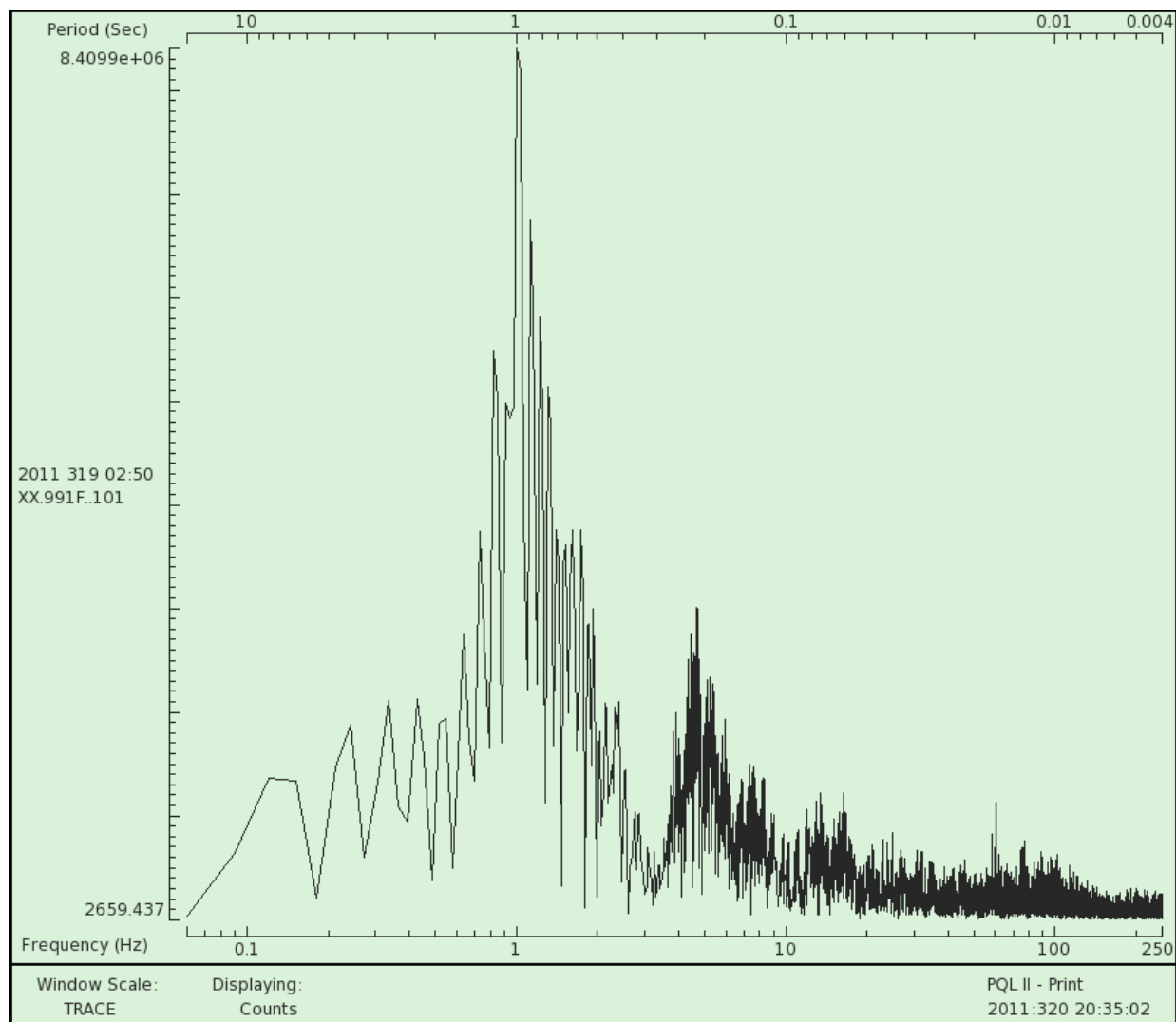


Fig. 11. The spectrum of a 4-5 sec time series of the sonobuoy record across one noise chirp showing a primary peak at 1 Hz.

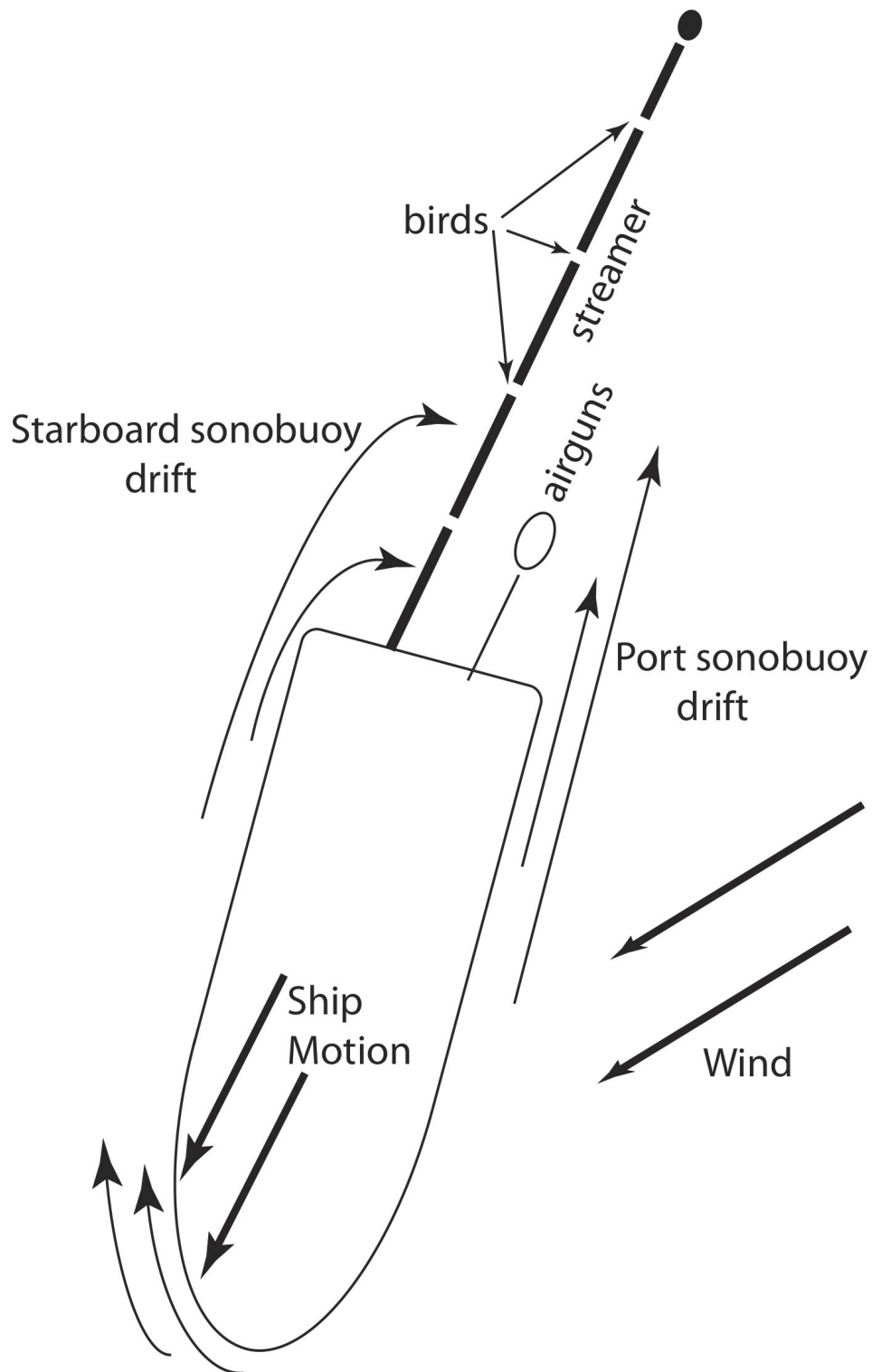


Fig. 12. A schematic diagram illustrates the hypothesis we came up with to explain the greater success of sonobuoys launched from port than from starboard. There is a greater flow of water around the starboard stern than the port due to the difference between the course steered and the course made good.

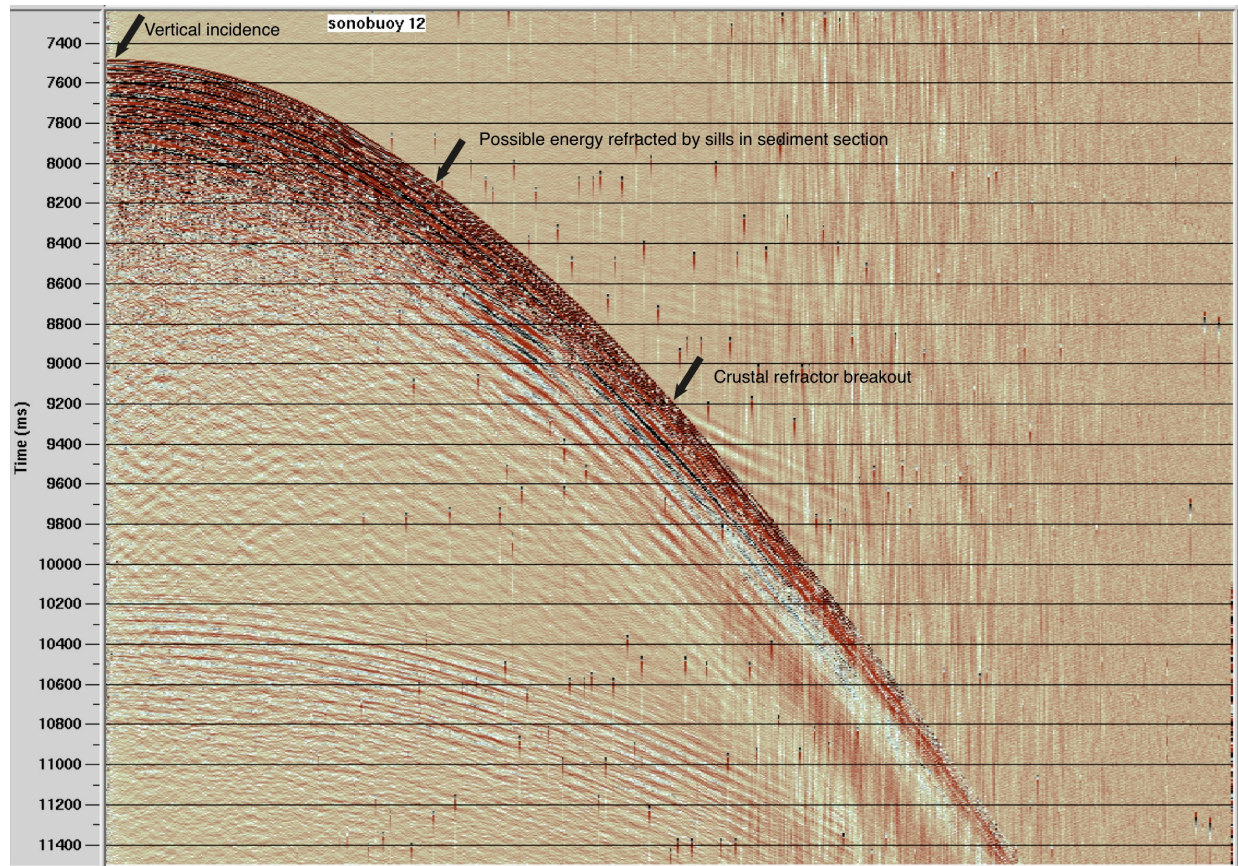


Fig. 13. Arrows on screen dump of the channel plot for sonobuoy 12 mark travel times picked for vertical incidence at close range and for the crustal breakout. The middle arrow points to the earliest breakout for faint energy at relatively high velocities that may represent energy refracted by igneous sills within the sediment layer.

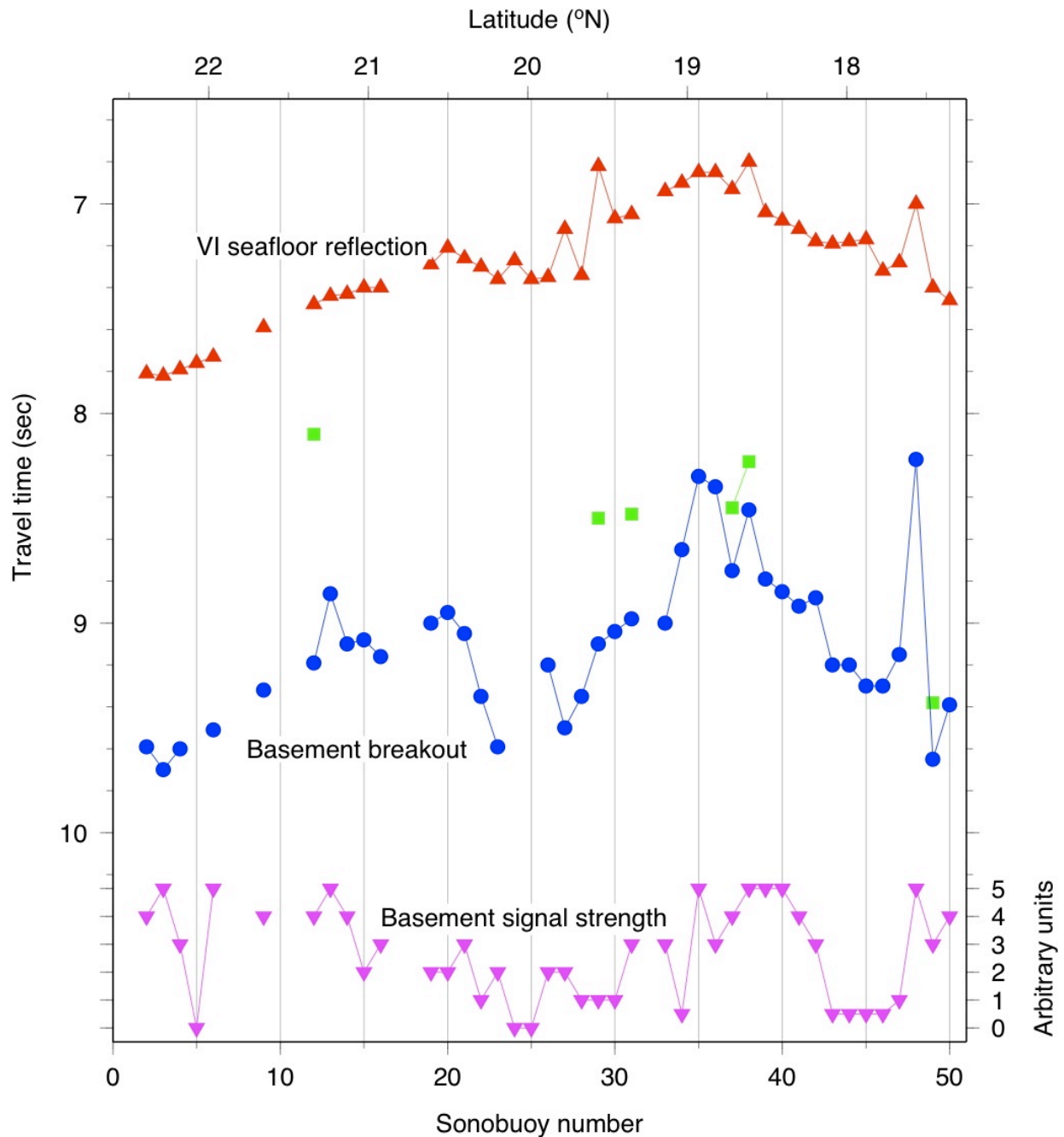


Fig. 14. Travel times picked from the sonobuoy channel plots for vertical incidence (red) and the primary crustal breakout (blue) decrease to sonobuoys 35-38, which were launched just south of 19°N where the survey line crosses through the gap in seamounts. Faint secondary breakouts from (green) were identified for six buoys. An arbitrary estimate of the amplitude of the crustal breakout is plotted at the bottom. Values of zero indicate that no crustal arrivals could be detected in the unfiltered channel plots.

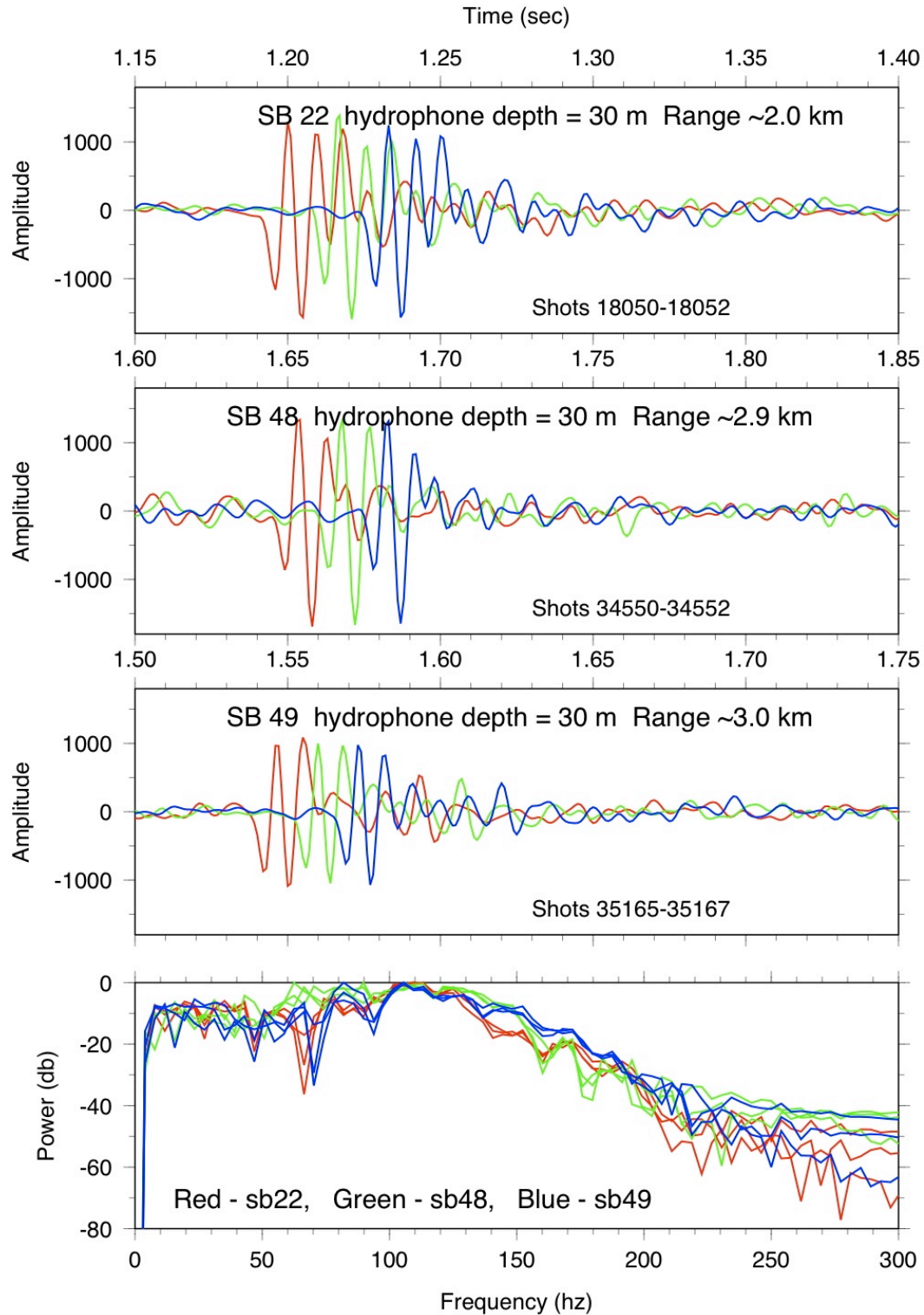


Fig. 15. We selected portions of the direct wave arrival from three sonobuoys for which noise levels were low both before and after the direct wave arrival. For each sonobuoy, the time series of three shots in sequence were plotted (red, green, and blue). In the bottom frame, colors indicate the sonobuoy number. Spectra, computed on 350 points padded to 512 points, peak at 100-110 Hz.

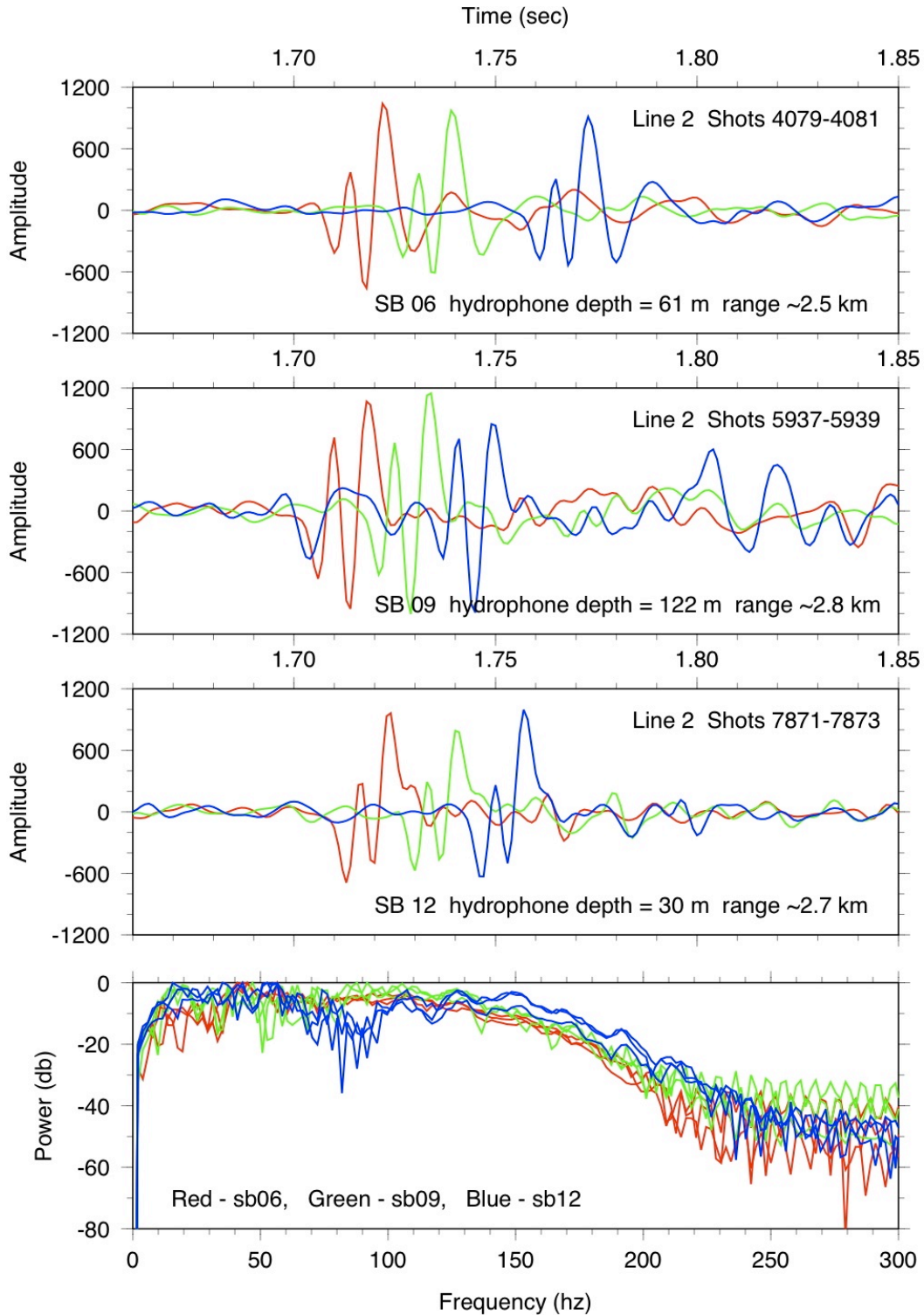


Fig. 16. We selected portions of the direct wave arrival from three sonobuoys for which the programmed hydrophone depth was 30, 61, or 122 m. Time series length and color coding are similar to that in Figure 15. The time series and spectra of SB #12 differ from not only the sonobuoys with deeper hydrophone depths in this figure but also from all the sonobuoys in Figure 15 with hydrophones at 30 m. Thus, it is likely that some parameter other than hydrophone depth most influences variability in the water-wave arrival.

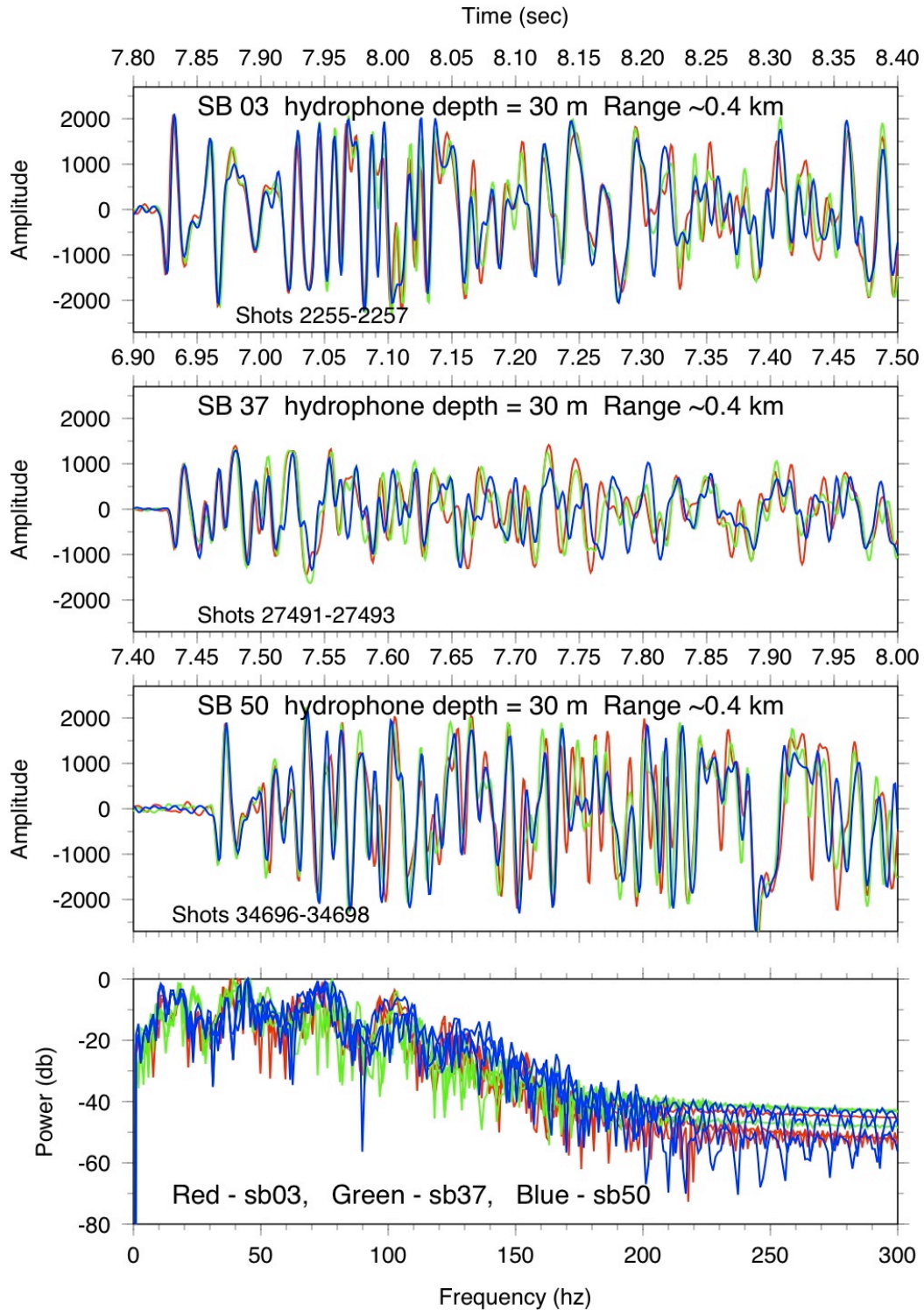


Fig. 17. To illustrate the time series and spectra of the seafloor reflections and sediment sequence, we selected three widely separated sonobuoys. Spectra were computed on 600 samples padded to 1024 points. The initial 30 ms reflection from the seafloor is nearly identical for all seismograms. The spectra are very similar despite the significant differences in sediment stratigraphy along the survey line.

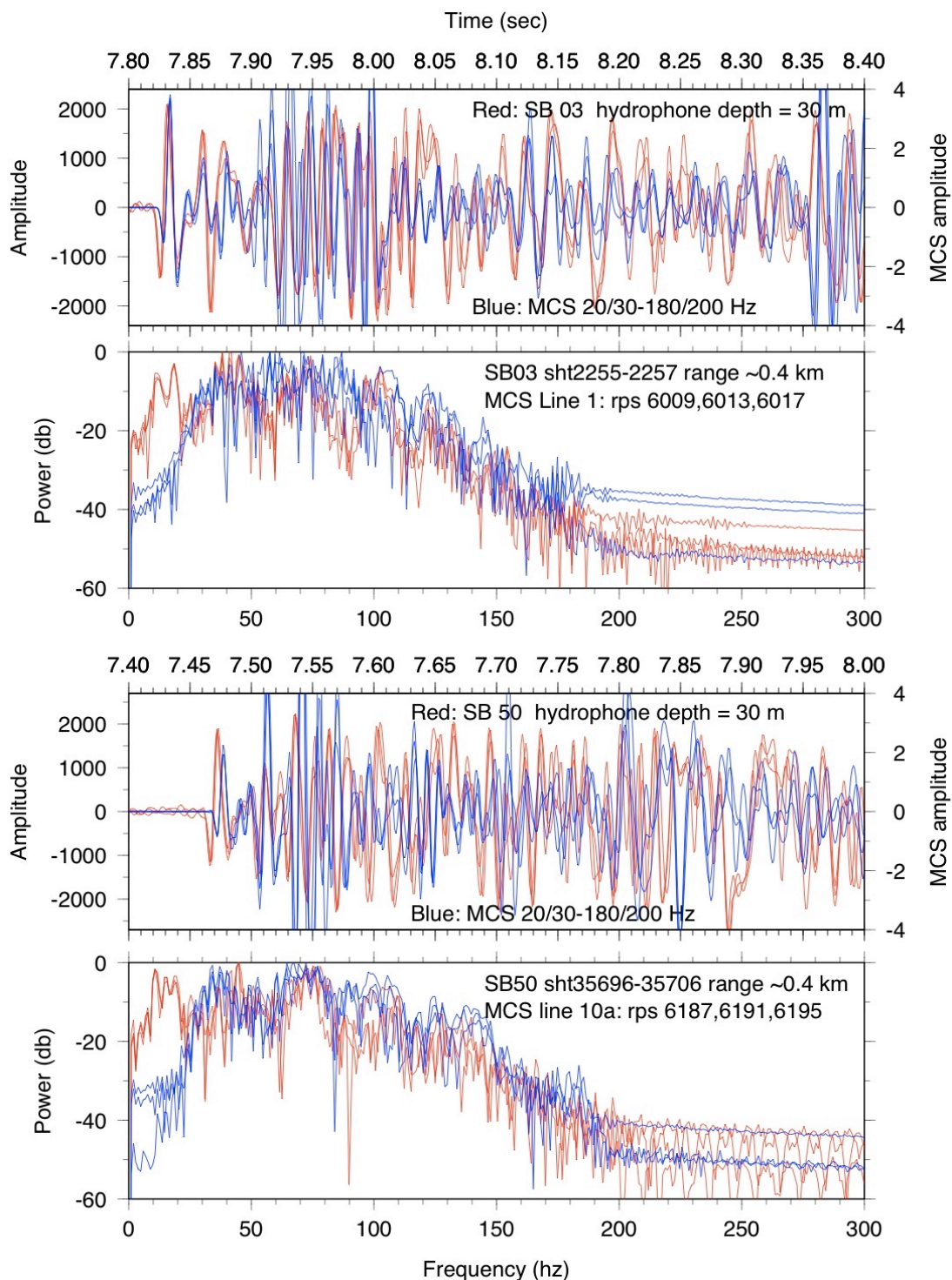


Fig. 18. Three traces recorded by both SB #3 and SB #50 at near-vertical incidence (red) are compared to “new” MCS traces with similar offset (blue). Phase relationships in the time series (upper frames) are remarkably similar, although reflections are more clearly imaged by MCS processing. Notches in the spectra appear in both sonobuoy and MCS traces and are aligned particularly well for SB #50 (lower frames). The spectra also illustrate the loss of low frequency energy caused by the bandpass filter applied during “new” MCS processing: 20/30-180/200 Hz.

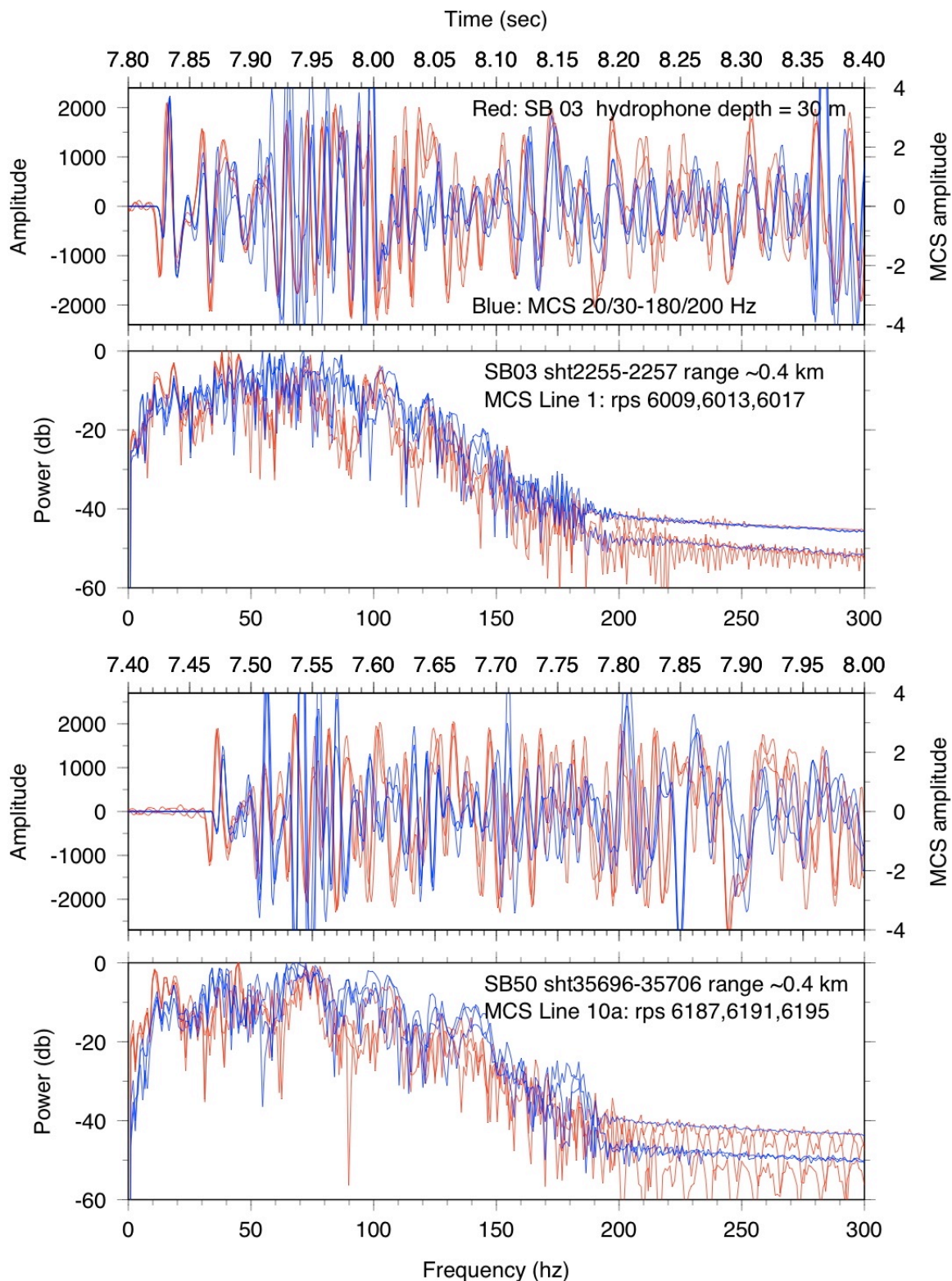


Fig. 19. Plots similar to those in Figure 18 except that the “final” MCS processing used a bandpass filter that was expanded to 5/8-180/200 Hz.

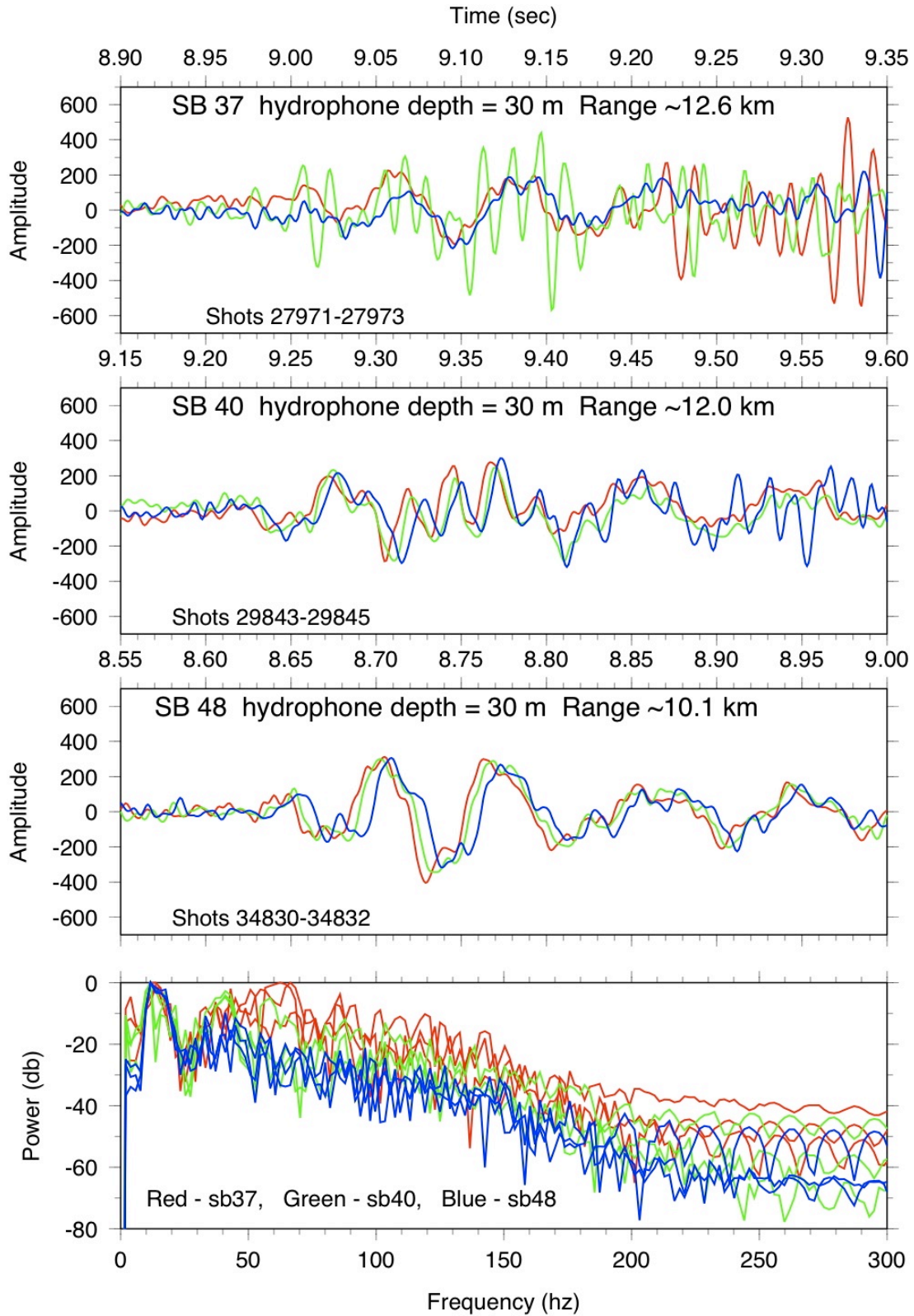


Fig. 20. Energy in crustal refractions arriving before the seafloor reflection in SBs 37, 40, and 48 is concentrated in the 10-15 Hz band.

Tables

Table 1 – XBT locations

Table 2 – Sentry dive locations

Table 3 – gps geometry from IMU

Table 4 – Sonobuoy status table

Table 5 – Sonobuoy deployment position, time, shot numbers

Table 1 – XBT locations

JD	Mo	Da	Yr	Hr	Min	Sec	Seq	Latitude	Longitude	probe	T-depth	ppt
309	11	05	2011	21	16	33	125	21.294068	-158.265217	T-5	1830	35.10
317	11	13	2011	23	27	15	126	23.295430	167.069272	F-D	1000	34.99
320	11	16	2011	19	14	50	127	22.119732	166.245628	F-D	1000	35.00
327	11	23	2011	08	09	07	128	22.062107	165.583258	F-D	1000	34.98
331	11	27	2011	02	09	41	129	20.677628	165.068487	F-D	1000	34.87
339	12	05	2011	17	54	05	130	19.365393	163.918067	T-5	1830	34.87
347	12	13	2011	04	36	22	133	18.437927	162.564982	T-5	1830	34.90

Table 2 – Sentry dive locations

Dive	Launch						Recovery					
	JD	Hr	Min	Sec	Latitude	Longitude	JD	Hr	Min	Sec	Latitude	Longitude
127	311	14	07	28	18.3546	163.2794	311	23	15	37	18.3571	163.2549
128	319	08	53	07	22.5813	166.6443	320	19	29	11	22.1213	166.2450
129	325	16	18	32	22.1428	166.2900	326	18	51	00	22.0468	166.1676
130	331	00	38	14	20.6780	165.0667	331	02	45	37	20.6785	165.0651
131	334	10	02	02	17.1908	161.5529	334	13	24	25	17.1704	161.5392
132	336	05	02	30	20.6777	165.0687	336	15	53	49	20.7564	165.1364
133	341	01	17	50	18.6669	163.0374	341	19	20	35	18.8616	163.2193
134	342	23	14	06	18.2666	162.6333	344	08	39	02	18.6830	163.0290

Table 3 – gps geometry from IMU

Location	Frame Number	Offset from C/L (m)	Fore-aft offset from IMU (m)	Star-port offset from IMU (m)
IMU	53	-1.5	0.0	0.0
PosMV GPS			0.0	0.0
Cnav GPS			-5.0	+1.3
Mast	62	0.0	-4.6	+1.3
Sonobuoy GPS	91	-1.0	-23.2	+0.5
Sonobuoy antenna	56	+6.1	-1.8	+7.6
Sonobuoy launch positions				
SB 1-3 starboard main deck	103	+7.9	-30.5	+9.4
SB 4-5 starboard 02 deck	50	+7.3	+1.8	+8.8
SB 6 starboard bridge deck	58	+7.9	-3.0	+9.4
SB 7-18 starboard 02 deck	50	+7.3	+1.8	+8.8
SB 19-50 port 02 deck	57	-7.3	-2.4	-5.8

Table 4 – Sonobuoy status table

Buoy	Line	Mon	Day	JD	S/N	Chan	Freq	Hydro Depth	Launch				End Time	
								(m)	Time	Lat	Lon	Depth		
1	1	11	14	318	620-026	33	136.375	30	19:19:34	22 34.5015	166 38.4138	5961	21:26:19	G?
2	1	11	14	318	620-014	35	137.125	30	21:27:15	22 28.3661	166 33.4045	5925	23:44:45	G
3	1	11	14	318	620-024	39	138.625	30	23:45:53	22 21.1862	166 27.5649	5927	00:01:52	G
4	1	11	15	319	620-032	33	136.375	30	01:53:27	22 14.3560	166 22.0270	5901	03:33:01	G
5	2	11	16	320	620-009	33	136.375	61	22:13:20	22 10.0067	166 18.5087	5890	00:23:53	G
6	2	11	17	321	620-033	39	138.625	61	00:24:32	22 02.8535	166 13.1203	5877	02:41:56	G
7	2	11	17	321	620-035	43	140.125	61	02:40:30	21 55.6939	166 07.7376	5855	05:00:20	NG
8	2	11	17	321	620-040	45	140.875	61	05:02:48	21 48.8271	166 01.5236	5760	07:21:26	NG
9	2	11	17	321	620-047	48	142.000	122	07:23:20	21 42.1886	165 55.0782	5785	09:41:10	G
10	2	11	17	321	620-016	35	137.125	61	09:43:44	21 35.5333	165 50.1282	5911	11:59:07	NG
11	2	11	17	321	620-029	41	139.375	122	12:01:28	21 29.1036	165 44.7130	5825	14:29:05	NG
12	2	11	17	321	620-028	32	136.000	30	14:31:06	21 21.7649	165 38.5778	5723	16:34:40	G
13	2	11	17	321	620-013	40	139.000	30	16:41:42	21 15.1651	165 33.0753	5672	18:58:05	G
14	2	11	17	321	620-021	44	140.500	30	18:59:41	21 08.2845	165 27.2368	5963	21:08:30	G
15	2	11	17	321	620-015	47	141.625	30	21:11:34	21 01.7343	165 21.7477	5670	23:31:58	G
16	2	11	17	321	620-031	34	136.750	30	23:35:15	20 54.9082	165 16.0467	5691	01:44:01	G
17	2	11	18	322	620-003	42	139.750	30	01:51:37	20 48.1393	165 10.3833	5697	04:12:00	NG
18	7	11	27	331	620-022	32	136.000	30	05:11:58	20 39.9564	165 03.6876	5547	06:55:00	NG
19	7	11	27	331	620-038	35	137.125	30	06:59:00	20 34.2300	164 59.4100	5505	09:06:00	G
20	7	11	27	331	620-034	38	138.250	30	09:07:45	20 27.3262	164 54.3091	5445	11:15:00	G
21	7	11	27	331	620-007	41	139.375	30	11:17:00	20 20.2840	164 49.1350	5486	13:31:45	G
22	7	11	27	331	620-043	44	140.500	30	13:32:31	20 13.2199	164 43.9207	5523	15:46:00	G
23	7	11	27	331	620-027	47	141.625	30	15:50:36	20 05.9495	164 38.5838	5564	18:02:00	G
24	7	11	27	331	620-045	33	136.375	61	18:06:01	19 58.8992	164 33.3545	5515	20:32:06	G
25	7/8	11	27	331	620-042	36	137.500	61	20:33:16	19 50.9387	164 27.2961	5582	22:26:00	G
26	8	11	27	331	620-008	39	138.625	30	22:27:15	19 45.9103	164 21.7608	5557	00:37:00	G
27	8	11	28	332	620-041	42	139.750	30	00:43:42	19 39.9294	164 15.1460	5377	02:58:00	G

Buoy	Line	Mon	Day	JD	S/N	Chan	Freq	Hydro Depth	Launch				End Time	
								(m)	Time	Lat	Lon	Depth		
28	8	11	28	332	620-004	45	140.875	30	02:59:35	19 33.0073	164 08.5629	5543	05:12:00	G
29	8	11	28	332	620-018	48	142.000	61	05:12:58	19 28.1408	164 02.0884	5346	07:25:00	G
30	8	11	28	332	620-010	34	136.750	30	07:27:17	19 22.1743	163 55.5051	5335	09:50:00	G
31	8	11	28	332	620-049	37	137.875	30	09:52:00	19 15.9110	163 48.6570	5326	12:00:00	G
32	8	11	28	332	620-048	40	139.000	30	12:02:00	19 10.2117	163 42.3680	5303	14:08:00	NG
33	8	11	28	332	620-036	43	140.125	30	14:12:20	19 04.3513	163 35.9499	5239	16:33:00	G
34	8	11	28	332	620-050	46	141.250	30	16:39:47	18 57.7739	163 28.7798	5204	18:49:00	G
35	8	11	28	332	620-039	32	136.000	30	18:51:36	18 51.8570	163 22.3093	5172	20:54:00	G
36	8/9	11	28	332	620-006	35	137.125	30	20:56:00	18 46.0516	163 15.9721	5162	23:17:00	G
37	9	11	28	332	620-023	38	138.250	30	23:17:47	18 39.7837	163 09.1880	5228	01:31:00	G
38	9	11	29	333	620-030	41	139.375	30	01:29:15	18 33.9221	163 02.8354	5169	03:43:00	G
39	9	11	29	333	620-046	44	140.500	30	03:45:01	18 27.8618	162 56.2072	5319	05:57:45	G
40	9	11	29	333	620-019	47	141.625	30	05:58:53	18 21.9211	162 49.8016	5353	08:20:18	G
41	9	11	29	333	620-017	33	136.375	30	08:21:33	18 15.7171	162 43.0859	5376	10:39:00	G
42	9	11	29	333	620-012	36	137.500	30	10:40:50	18 09.8590	162 36.8309	5422	13:00:00	G
43	10	11	29	333	620-025	39	138.625	30	13:01:49	18 03.7836	162 30.3134	5434	15:17:30	G
44	10	11	29	333	620-053	42	139.750	30	15:19:18	17 57.6860	162 23.6923	5419	17:33:00	G
45	10	11	29	333	620-002	45	140.875	30	17:34:51	17 51.6503	162 17.2328	5427	19:47:45	G
46	10	11	29	333	620-037	48	142.000	30	19:49:07	17 45.4921	162 10.6320	5529	21:58:00	G
47	10	11	29	333	620-001	34	136.750	30	21:59:26	17 39.5085	162 04.2680	5507	01:15:51	G
48	10	11	30	334	620-005	37	137.875	30	00:17:05	17 33.5878	161 57.9888	5292	02:28:10	G
49	10	11	30	334	620-020	40	139.000	30	02:29:01	17 27.7246	161 51.7020	5601	04:39:50	G
50	10	11	30	334	620-011	43	140.125	30	04:42:22	17 21.6538	161 45.2278	5643	08:01:04	G

Table 5 – Sonobuoy deployment position, time, shot numbers

SB No	Start							End							Comments
	Day	JD	Hr	Min	Sec	Line	Shot No	Day	JD	Hr	Min	Sec	Line	Shot No	
1	14	318	19	19	34	1	1017	14	318	21	26	19	1	1570	
2	14	318	21	27	15	1	1575	14	318	23	44	45	1	2234	
3	14	318	23	45	53	1	2240	15	319	01	52	00	1	2840	
4	15	319	01	53	27	1	2857	15	319	03	33	01	1	3327	
5	16	320	22	13	20	2	3347	17	321	00	23	53	2	3975	
6	17	321	00	24	32	2	3979	17	321	02	41	56	2	4621	
7	17	321	02	40	30	2	4622	17	321	05	00	20	2	5185	Hydrophone cut. ~17 min time gap in shooting beginning 04:43:28
8	17	321	05	02	48	2	5194	17	321	07	21	26	2	5817	Hydrophone cut
9	17	321	07	23	20	2	5826	17	321	09	41	10	2	6438	
10	17	321	09	43	44	2	6450	17	321	11	59	07	2	7042	Hydrophone cut
11	17	321	12	01	28	2	7054	17	321	14	29	05	2	7753	Hydrophone cut
12	17	321	14	31	06	2	7763	17	321	16	34	40	2	8356	
13	17	321	16	41	42	2	8390	17	321	18	58	05	2	9044	
14	17	321	18	59	41	2	9053	17	321	21	08	30	2	9670	
15	17	321	21	11	34	2	9686	17	321	23	31	58	2	10359	
16	17	321	23	35	15	2	10375	18	322	01	44	01	2	10992	
17	18	322	01	51	37	2	11030	18	322	04	12	00	2	11703	Hydrophone cut
18	27	331	05	11	58	7	15572	27	331	06	58	00	7	16078	Hydrophone cut
19	27	331	06	59	00	7	16084	27	331	09	06	00	7	16695	
20	27	331	09	07	45	7	16705	27	331	11	15	00	7	17323	
21	27	331	11	17	00	7	17334	27	331	13	31	45	7	17968	
22	27	331	13	32	31	7	17972	27	331	15	49	00	7	18595	4 min time gap in shooting beginning 14:05:49
SB No	Start							End							Comments
	Day	JD	Hr	Min	Sec	Line	Shot No	Day	JD	Hr	Min	Sec	Line	Shot No	
23	27	331	15	50	37	7	18604	27	331	18	05	00	7	19232	
24	27	331	18	06	01	7	19238	27	331	20	32	06	7	19941	
25	27	331	20	33	16	7	19947	27	331	22	26	00	8	20471	C/C before start. Shots missed in MCS beginning 21:55:22 – Line 7/8 change
26	27	331	22	27	15	8	20478	28	332	00	37	00	8	21084	
27	28	332	00	43	42	8	21117	28	332	02	58	00	8	21744	
28	28	332	02	59	35	8	21752	28	332	05	12	00	8	22372	
29	28	332	05	12	58	8	22377	28	332	07	25	00	8	23003	
30	28	332	07	27	17	8	23015	28	332	09	50	00	8	23667	
31	28	332	09	52	00	8	23677	28	332	12	00	00	8	24272	
32	28	332	12	02	00	8	24283	28	332	14	08	00	8	24886	No signal – Dud
33	28	332	14	12	20	8	24908	28	332	16	33	00	8	25571	
34	28	332	16	39	47	8	25605	28	332	18	49	00	8	26210	
35	28	332	18	51	36	8	26223	28	332	20	54	00	8	26810	
36	28	332	20	56	00	8	26820	28	332	23	17	00	9	27471	Time gap in MCS at line 8/9 change beginning 21:27:55
37	28	332	23	17	47	9	27476	29	333	01	31	30	9	28096	
38	29	333	01	29	15	9	28097	29	333	03	43	00	9	28726	
39	29	333	03	46	01	9	28741	29	333	05	57	45	9	29361	
40	29	333	05	58	53	9	29368	29	333	08	20	18	9	30019	
41	29	333	08	21	33	9	30026	29	333	10	39	00	9	30635	
42	29	333	10	40	50	9	30644	29	333	13	00	00	10	31270	Recording gap at line 9/10 change 12:52:41
Start							End							Comments	

SB No	Day	JD	Hr	Min	Sec	Line	Shot No	Day	JD	Hr	Min	Sec	Line	Shot No	
43	29	333	13	01	49	10	31279	29	333	15	17	30	10	31916	
44	29	333	15	19	18	10	31925	29	333	17	33	00	10	32554	
45	29	333	17	34	51	10	32563	29	333	19	47	45	10	33203	
46	29	333	19	49	07	10	33210	29	333	21	58	00	10	33809	
47	29	333	21	59	26	10	33816	30	334	00	15	51	10	34429	Airgun failure at line 10/10a change ~7min sht gap beginning 00:00:30
48	30	334	00	17	05	10	34435	30	334	02	28	10	10	35041	
49	30	334	02	29	01	10	35046	30	335	04	39	50	10	35668	
50	30	334	04	42	22	10	35681	30	335	08	01	04	10	36573	Ends when guns shut off

Appendices

Appendix 1 – VHF antenna installation

Appendix 2 – GPS antenna installation

Appendix 3 – MCS geometry

Appendix 4 – Unprocessed sonobuoy record sections

Appendix 1 – VHF antenna installation







Appendix 2 – GPS antenna installation







Appendix 3 – MCS geometry

SIO Portable Marine Seismic System

Geometry 1

Tue, November 15, 2011
Lines 1 & 3-10

Cruise: TN272

Vessel: R/V Thompson

Date: Nov 2011

Chief Sci: Tominaga

Techs:

Lee Ellett
Jay Turnbull
Bridget Hass

Item or Channel	Distance (m) from Stern	Distance (m) from Source	Distance (m) From GPS	Distance (m) off center line	Depth/Height from water
1	101.25	76.25	126.25	2	4
48	688.75	663.75	713.75	2	4
Source	25	0	50	2	4
GPS	25	50	0	2	29

Section	Length (m)	Number of Channels
Towing Cables	95	
Active Sections	600	48
Tail Stretch and Rope	125	
Group Int	12.5	

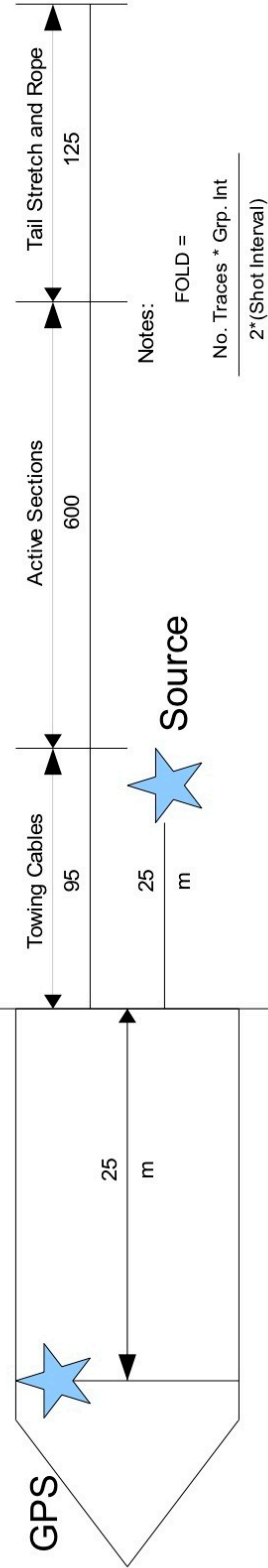
Auxiliary Channels

AUX 1	Gun Timebreak
AUX 2	Gun 1 Near Field
AUX 3	Gun 2 Near Field
AUX 4	Sonobuoy

Bird Locations

Bird 1	Start of Tow Stretch
Bird 2	Start of Ch 17 (Active 3)
Bird 3	Start of Ch 33 (Active 5)
Bird 4	Start of Tail Stretch

Source:	GI gun	105/105 Harmonic	Qty: 2
Acq. Sys.	GeoEel	PreAmp Gain:	18 db
Sample Int:	1 ms	# of Channels:	48
File Format:	SEGD	D 8058 Rev 1	
Rec. Length:	11.5 sec	Shot Interval:	25m



* Not drawn to Scale

SIO Portable Marine Seismic System

Geometry 2

Wed, November 16, 2011
Line 2

Cruise: TN272

Vessel: RV Thompson

Date: Nov 2011

Chief Sci: Tominaga

Techs:

Lee Ellett

Jay Turnbull

Bridget Hass

Item or Channel	Distance (m) from Stern	Distance (m) from Source	Distance (m) From GPS	Distance (m) off center line	Depth/Height from water
1	101.25	76.25	121.25	2	4
48	688.75	663.75	708.75	2	4
Source	25	0	45	2	4
GPS	20	45	0	2	29

Section	Length (m)	Number of Channels
Towing Cables	95	
Active Sections	600	48
Tail Stretch and Rope	125	
Group Int	12.5	

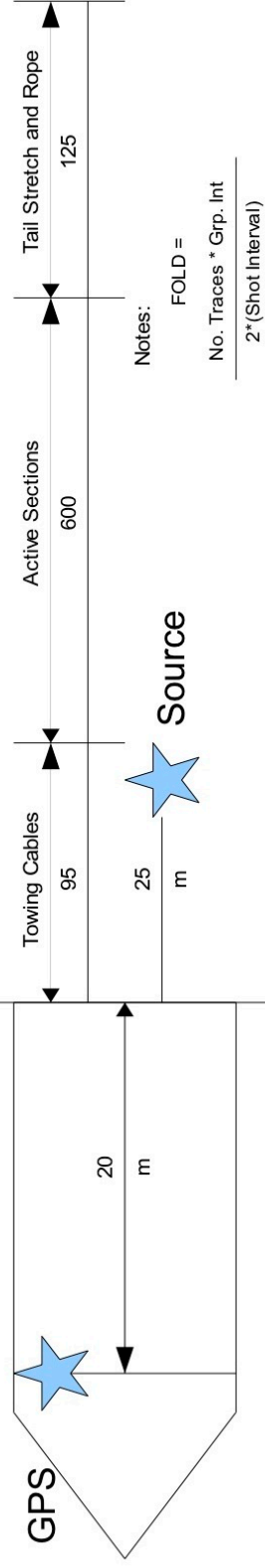
Auxiliary Channels

AUX 1	Gun Timebreak
AUX 2	Gun 1 Near Field
AUX 3	Gun 2 Near Field
AUX 4	Sonobuoy

Bird Locations

Bird 1	Start of Tow Stretch
Bird 2	Start of Ch 17 (Active 3)
Bird 3	Start of Ch 33 (Active 5)
Bird 4	Start of Tail Stretch

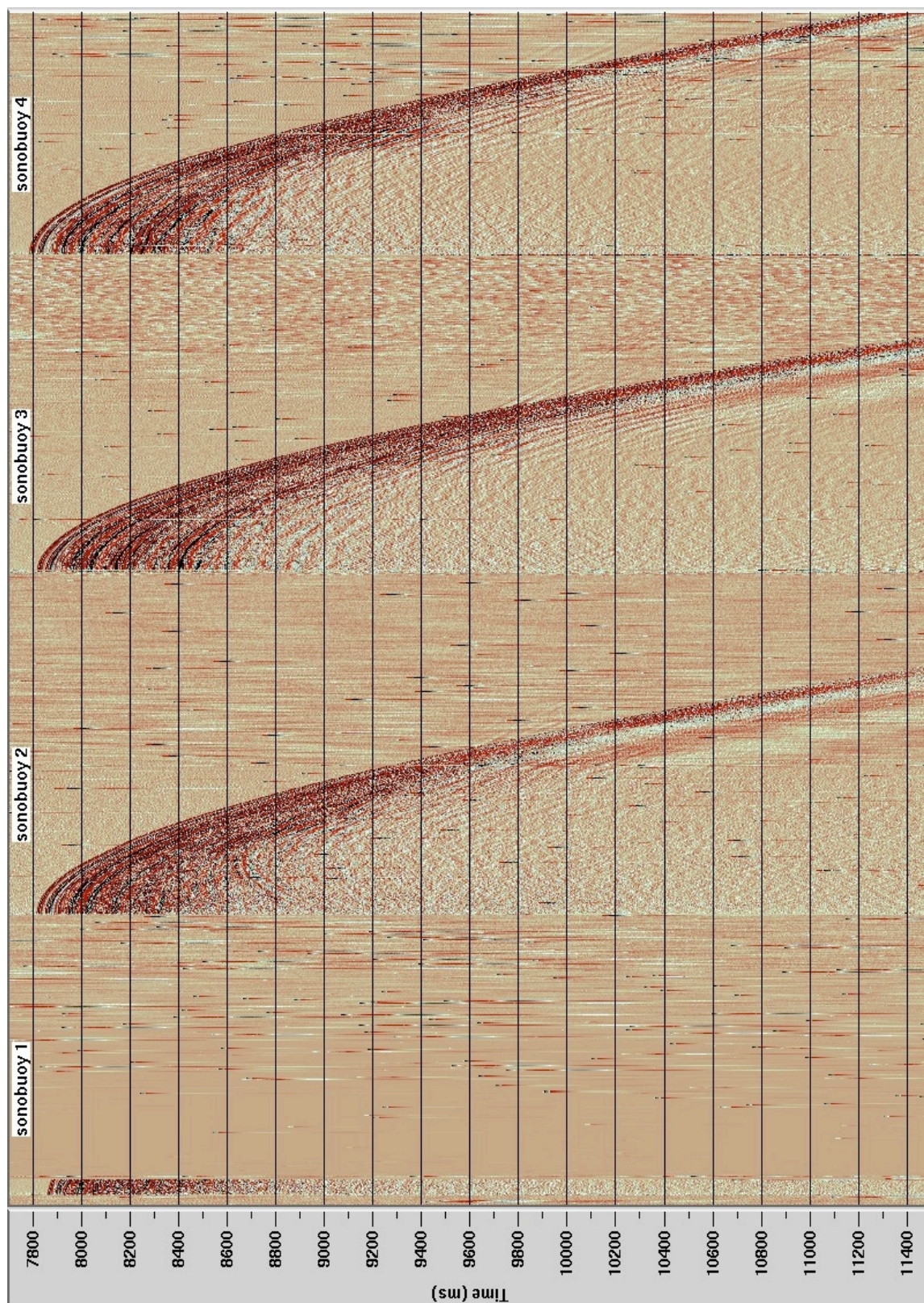
Source:	GI gun	105/105 Harmonic	Qty: 2
Acq. Sys.	GeoEel	PreAmp Gain:	18 db
Sample Int:	1 ms	# of Channels:	48
File Format:	SEGD	D 8058 Rev 1	
Rec. Length:	11.5 sec	Shot Interval:	25m



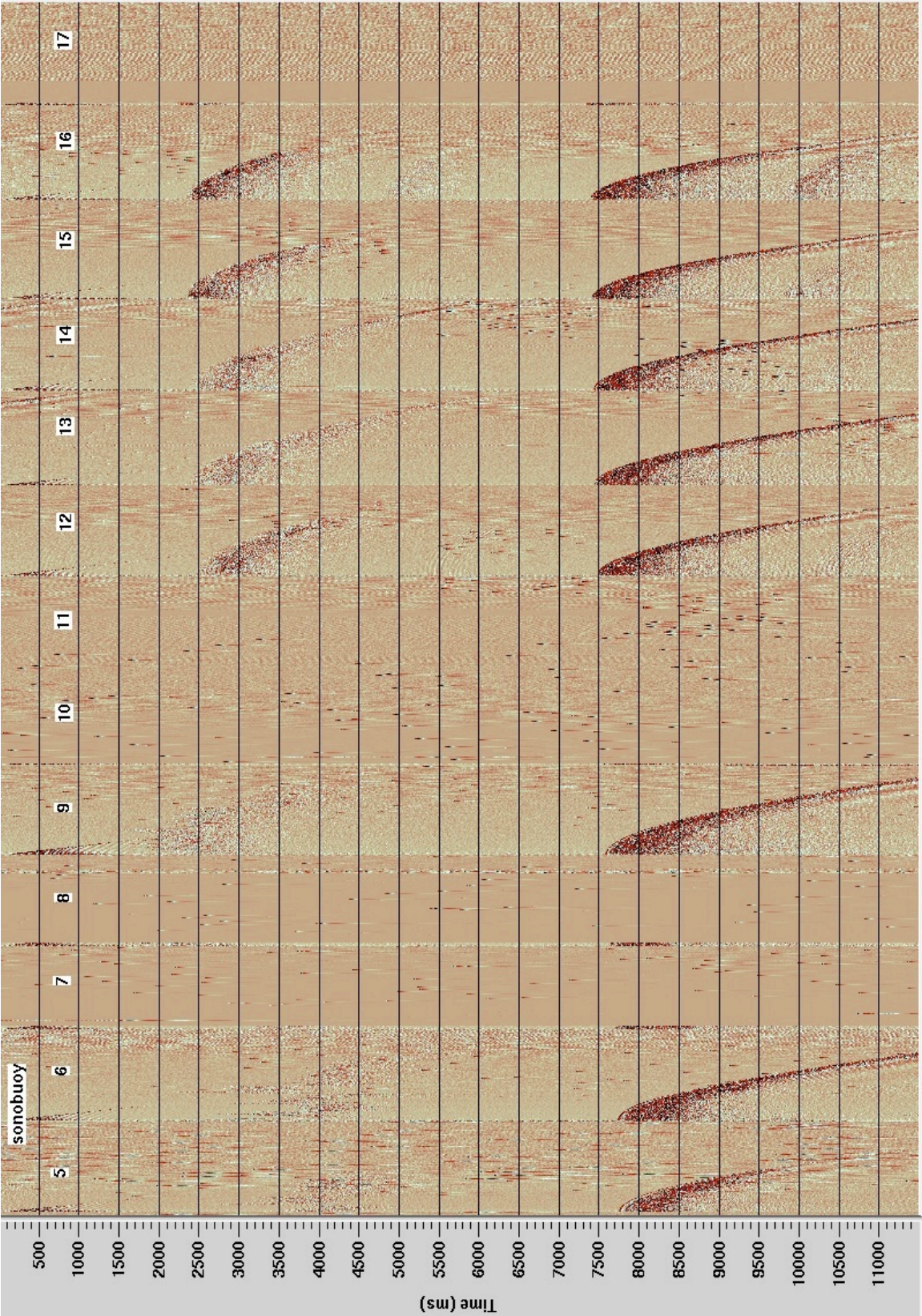
* Not drawn to Scale

Appendix 4 – Unprocessed sonobuoy record sections

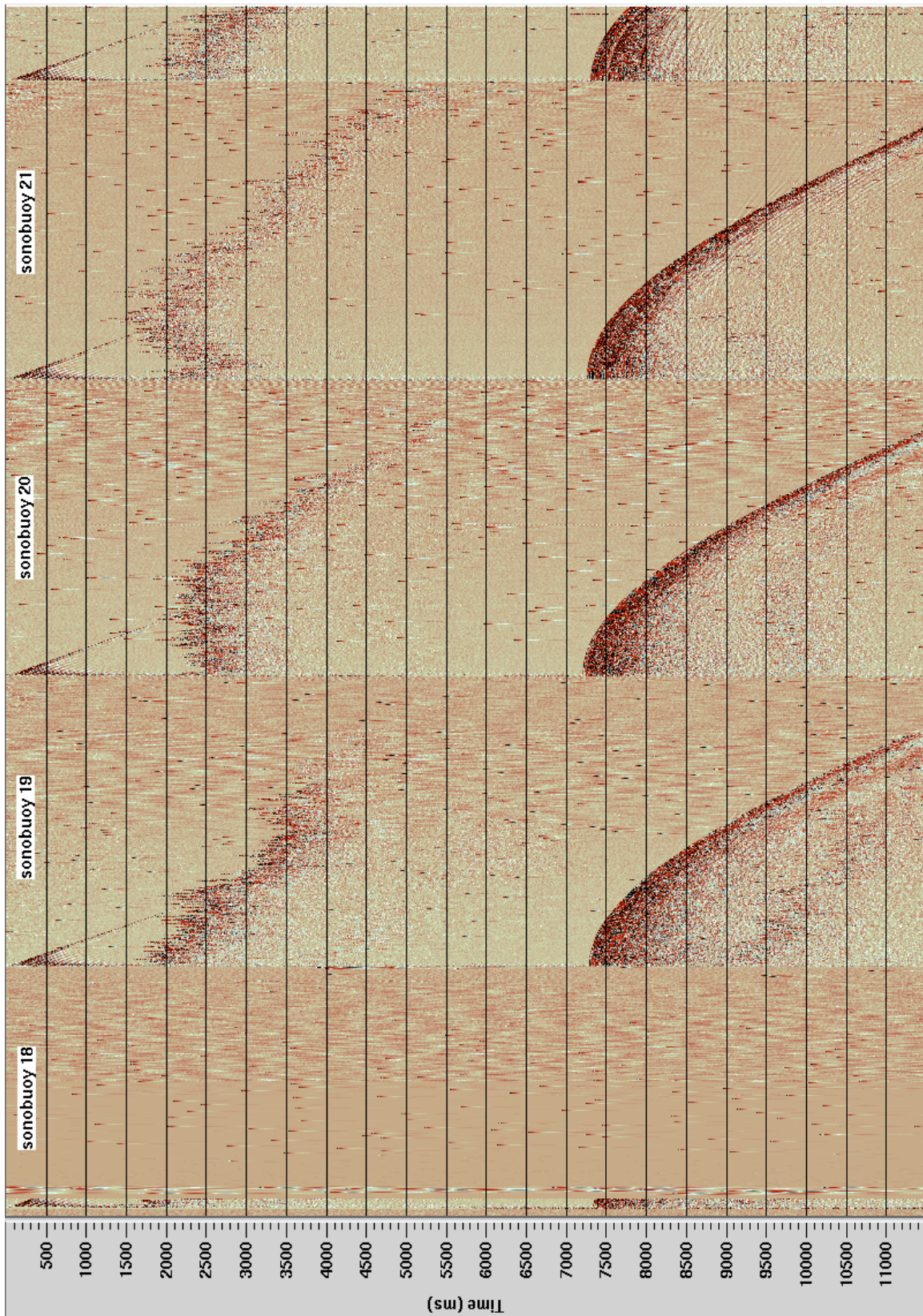
Line 1



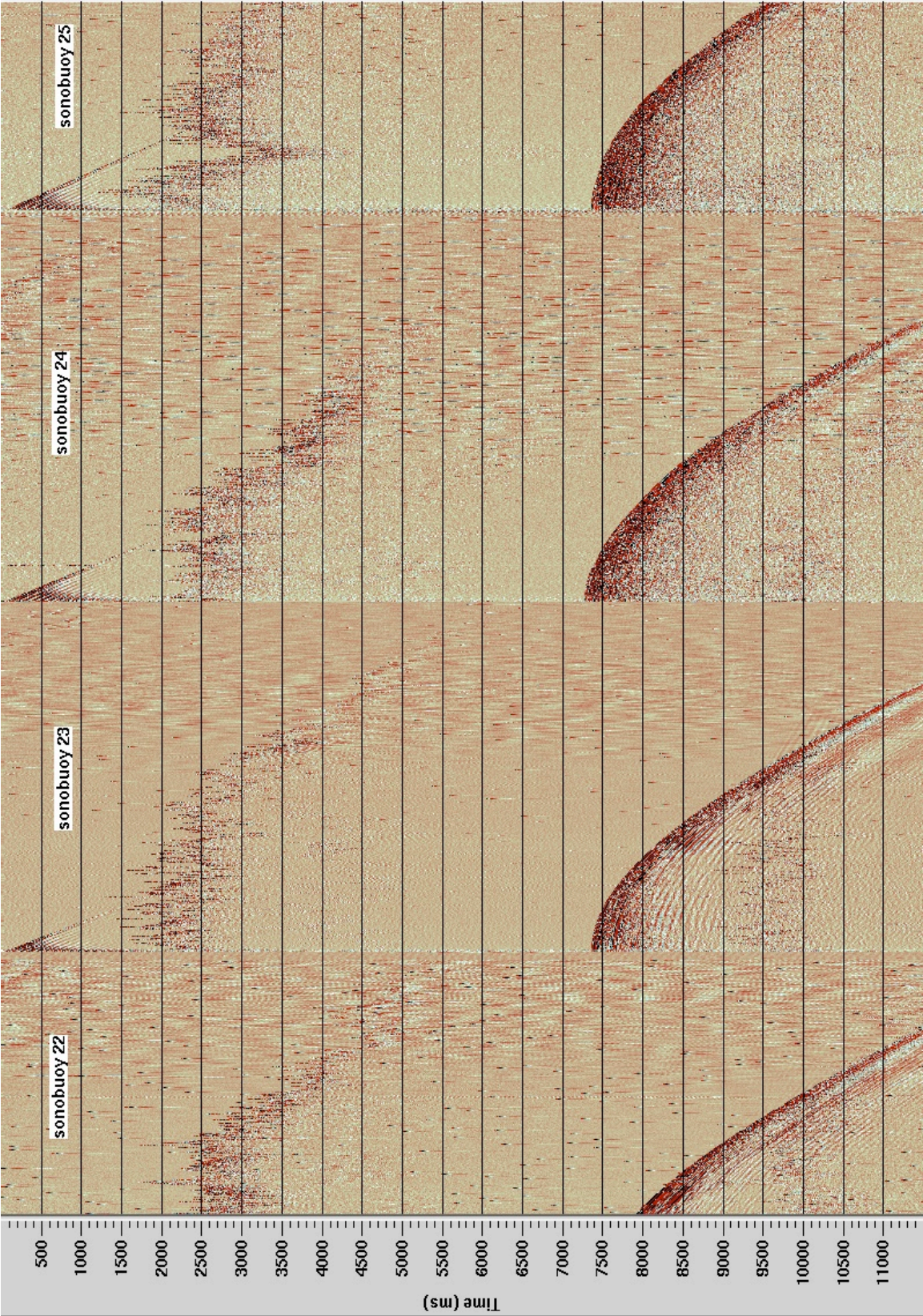
Line 2



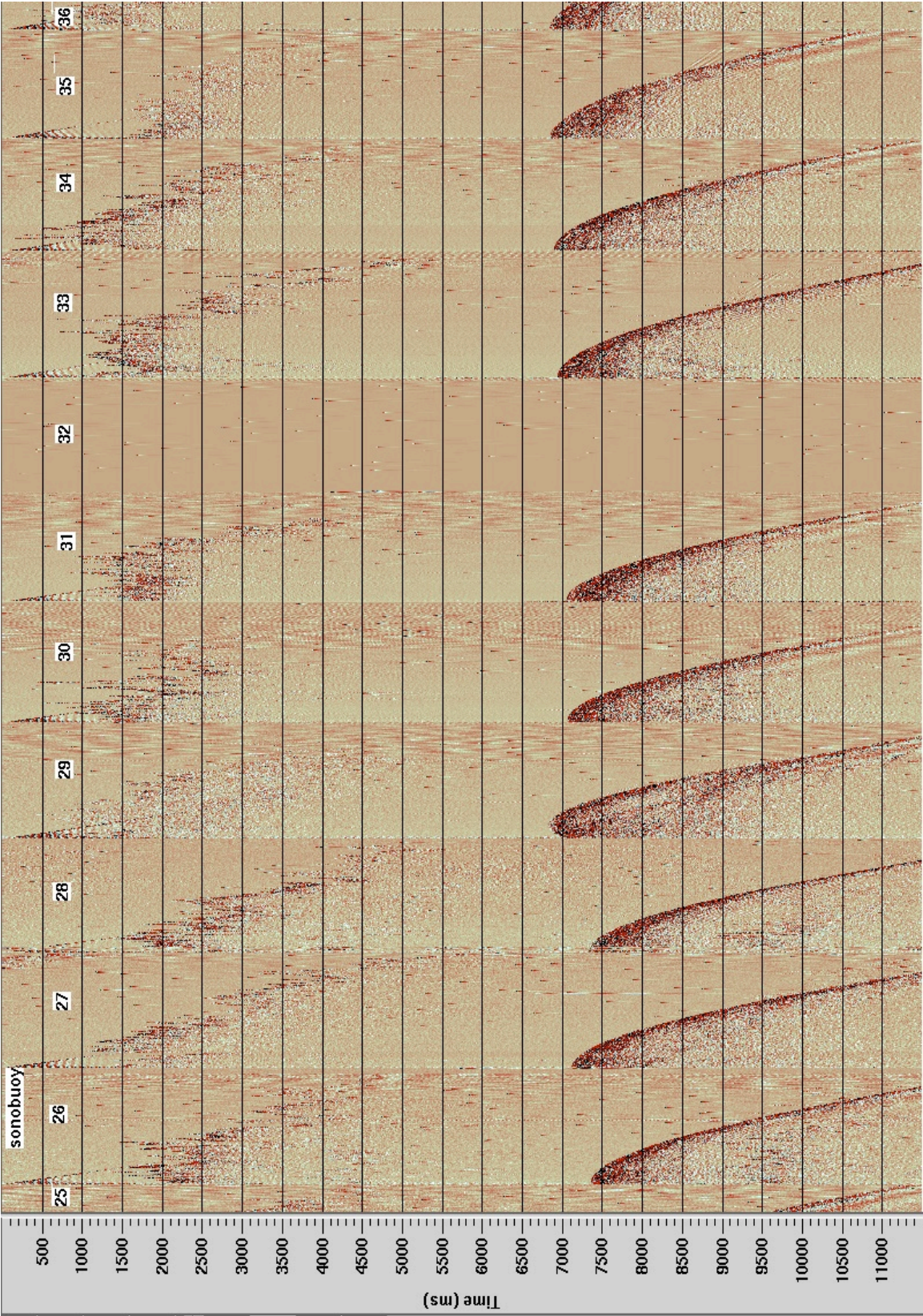
Line 7 part 1



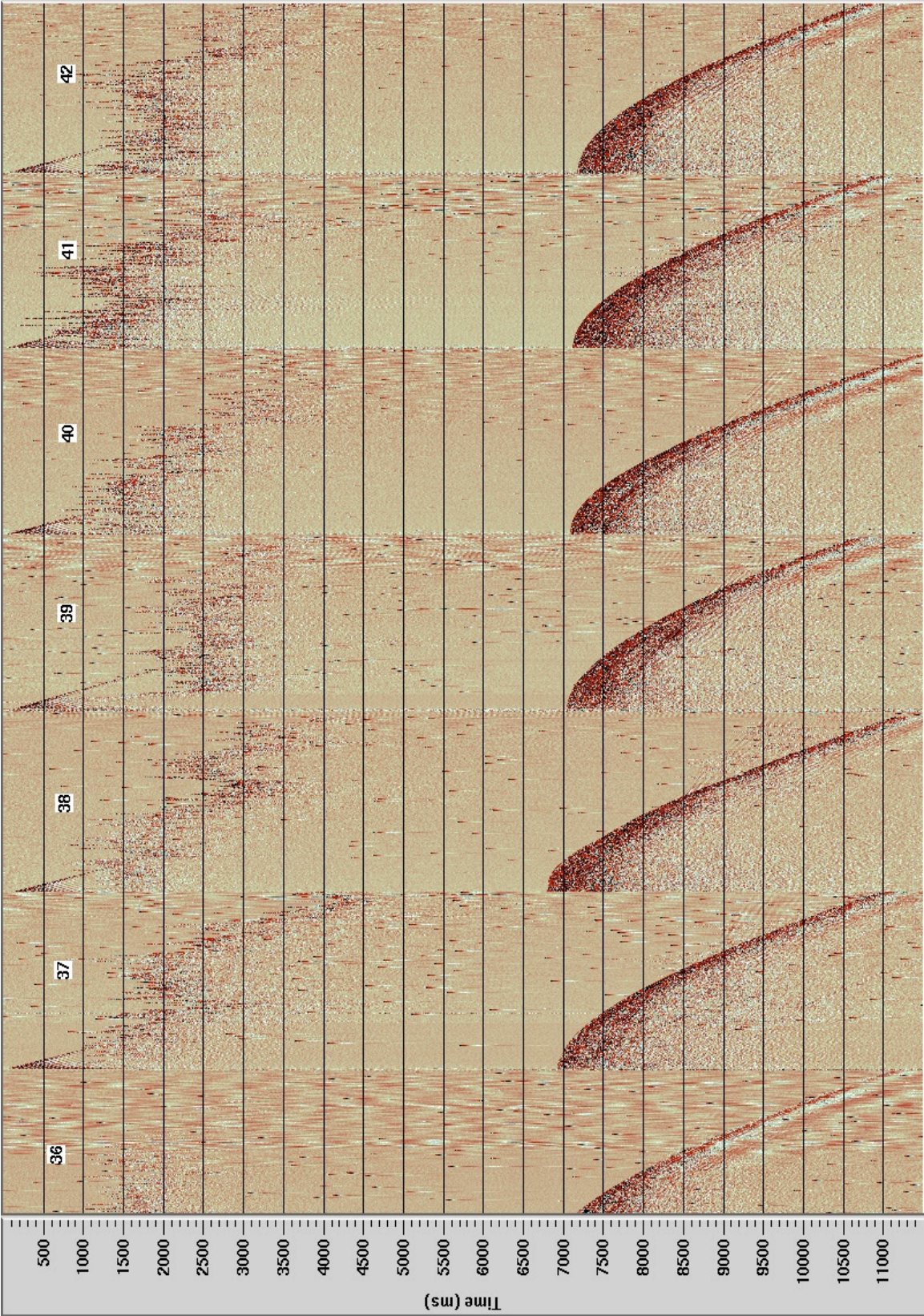
Line 7 part 2



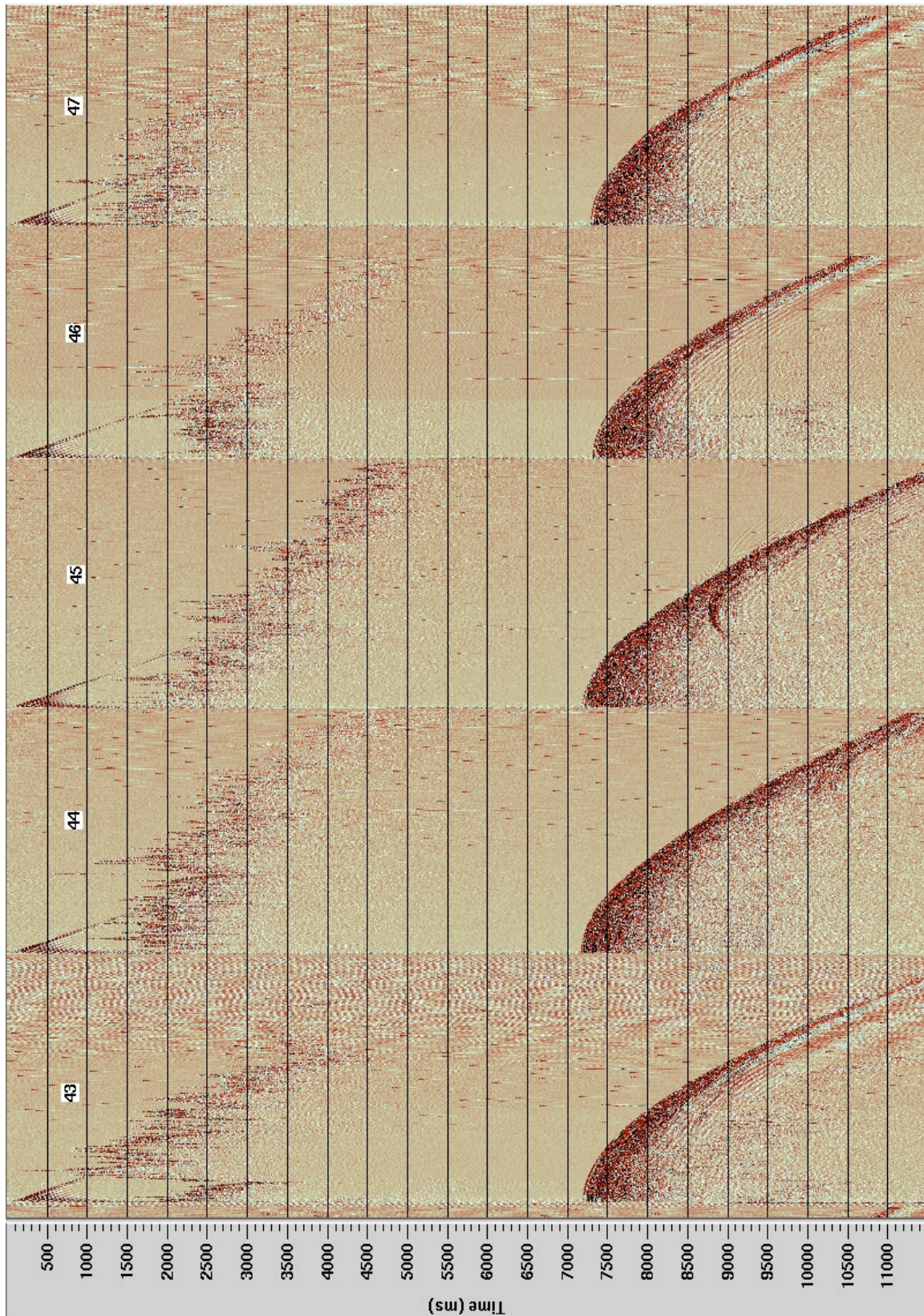
Line 8



Line 9



Line 10 (43-47)



Line 10 (48-50)

